New Remains of Camelus grattardi (Mammalia, Camelidae) from the Plio-Pleistocene of Ethiopia and the Phylogeny of the Genus

Denis Geraads, W. Andrew Barr, Denne Reed, Michel Laurin, Zeresenay Alemseged

New remains of *Camelus grattardi* (Mammalia, Camelidae) from the Plio-Pleistocene of Ethiopia and the phylogeny of the genus

By Denis Geraads[1,2*], W. Andrew Barr[3], Denne Reed[4], Michel Laurin[1], and Zeresenay Alemseged[5]

[1]CR2P-UMR 7207, CNRS, MNHN, UPMC, Sorbonne Universités, CP 38, 8 rue Buffon, 75231 Paris Cedex 05, France; denis.geraads@mnhn.fr; michel.laurin@mnhn.fr;

[2]Department of Human Evolution, Max Planck Institute for Evolutionary Anthropology, Deutscher Platz 6, 04103 Leipzig, Germany;

[3]Center for the Advanced Study of Human Paleobiology, Department of Anthropology, The George Washington University, Washington DC 20052, USA; wabarr@gmail.com;

[4]Department of Anthropology, University of Texas at Austin. Austin, TX 78712; USA; reedd@austin.utexas.edu

[5]Organismal Biology and Anatomy, University of Chicago, Chicago 60637, USA; alemseged@uchicago.edu;

* Corresponding author. ORCID id. 0000-0003-2475-8011

Running head: Plio-Pleistocene *Camelus* from Ethiopia

Abstract

The Old World fossil record of the family Camelidae is patchy, but a new partial cranium and some other remains of *Camelus grattardi* from the Mille-Logya Project area in the Afar, Ethiopia, greatly increase the fossil record of the genus in Africa. These new data – together with analysis of unpublished and recently published material from other sites, and reappraisal of poorly known taxa – allow for a comprehensive phylogenetic analysis showing that *C. grattardi* is the earliest (2.2–2.9

Ma) and most basal species of the genus. We also show that the lineages leading to the extant taxa *C. dromedarius* and *C. bactrianus* diverged much higher in the tree, suggesting a recent age for this divergence. A late divergence date between the extant species is consistent with the absence of any fossil forms that could be ancestral, or closely related, to any of the extant forms before the late Pleistocene, but stands in contrast to molecular estimates which place the divergence between the dromedary and the Bactrian camel between 8 and 4 million years ago.

Keywords: Mammalia, Camelidae, phylogeny, Pleistocene, Eastern Africa

Introduction

Most of the early evolution of Old World Camelidae, since their immigration from North America in the late Miocene (Honey et al. 1998; Harris et al. 2010; Rybczynski et al. 2013), seems to have occurred in Eurasia. Late Miocene and early Pliocene forms in Eurasia are usually referred to *Paracamelus* Schlosser, 1903, a genus that is currently diagnosed primarily by the retention of a lower third premolar, which is lost in the extant genus *Camelus* Linnaeus, 1758. *Paracamelus* has a wide distribution from Western Europe (Colombero et al. 2017) to China (Zdansky 1926; Teilhard de Chardin and Trassaert 1937) and through Eastern Europe (Ştefănescu 1895; Khaveson 1954; Kozhamkulova 1986; Logvynenko 2001), but remains very incompletely described. In Africa, it is documented by scrappy remains from the Pliocene of Chad, Tunisia, and Egypt (Harris et al. 2010). Fossil *Camelus* are also poorly known. The fragmentary remains from the Plio-Pleistocene of Omo-Turkana Basin of Kenya and Ethiopia (Howell et al. 1969; Grattard et al. 1976; Harris et al. 2010) have been assigned to *C. grattardi* Geraads, 2014 (Geraads 2014; Rowan et al. 2018), whose type-specimen is from Member G of the Omo Shungura Formation, dated to 2.2 Ma. Until now, the only fossil camel cranium known in Africa was from the late early Pleistocene of Tighennif, Algeria, which is the type locality of *C. thomasi* Pomel, 1893 (Martini and Geraads 2018).

In 2014, the Mille-Logya Project (MLP) discovered a relatively complete cranium in the upper Pliocene sediments of the Mille-Logya area, Lower Awash Valley, Ethiopia. Its characters match those of the type-specimen of *C. grattardi*, and we assign it to this species. In addition to considerably expanding the hypodigm of *C. grattardi*, the newly discovered cranium, together with a few additional isolated teeth and postcranial remains from the same stratigraphic unit, allow us to assess the phylogeny of the genus.

All data for this article are included in the following text and in the Supplementary Information. Anatomical terminology is translated from Latin, following the World Association of Veterinary Anatomists (1973).

Geological setting

The Mille-Logya Project (MLP), led by one of us (ZA), has conducted research in the Lower Awash Valley of Ethiopia since 2012. Sediments in this area date to c.a. 3 – 2.4 Ma and largely post-date the Hadar Formation exposed at several nearby sites (Alemseged et al. 2016). The fossil fauna from the new research area, currently under study, is diverse. The abundance of presumably grazing equids and alcelaphin bovids at MLP suggests a relatively open environment with extensive grass cover, as in the nearby Ledi-Geraru sequence (Rowan et al. 2016; Bibi et al. 2017; Robinson et al. 2017), but is not consistent with the sub-desertic environments favored by extant camels. The camel cranium described here (NME-MLP-1346), as well as the additional isolated teeth and postcranial remains, are all from the Seraitu unit dated to c. 2.5 − 2.9 Ma. All MLP fossils described here are housed in the National Museum of Ethiopia, Addis Ababa (NME).

Old World Camelidae

We compared the MLP fossils to a large sample of extant camels, especially skulls: *C. bactrianus* Linnaeus, 1758 (17 skulls; we include here the so-called *C. ferus* Przewalski, 1878, as there is no evidence that the two species can be distinguished morphologically); *C. dromedarius* Linnaeus, 1758 (34 skulls); hybrids or unidentified (4 skulls), housed in Muséum National d'Histoire Naturelle, Paris (MNHN), Centre de Conservation et d'Etude des Collections, Lyon (CCEC), and Zoological Institute, Saint Petersburg (ZIN). The distinction between extant species has recently been fully analyzed (Martini et al. 2017). In addition, we have examined the following fossil forms:

1. *Camelus sivalensis* Falconer and Cautley, 1836, from the upper Siwaliks (Falconer and Cautley 1846; Colbert 1935; Nanda 1978; Gaur et al. 1984), housed in the Natural History Museum, London (NHMUK) and American Museum of Natural History, New York (AMNH); R. Patnaik was kind enough to provide us with photos of the relatively complete cranium A/646 (Sahni and Khan 1988). It was the first fossil camel species to be described,

and is also the best represented in collections. Its appearance in the upper Siwaliks is dated at 2.6 Ma, or perhaps slightly older (Patnaik 2013). It differs from extant forms in its supraorbital foramina that open wider apart, more complete P3 lingual crescent, broader molars with stronger ribs and styles, more oblique ramus of the mandible, and the shorter ligament scars on the proximal phalanges.

2. The type-cranium of the Middle Pleistocene *C. knoblochi* Nehring, 1901 (ZIN-8678/8679), a few specimens of the same species from Sjara-Osso-Gol (Boule et al. 1928), stored in MNHN, complemented with photos of other specimens, kindly provided by V. Titov (cranium from Razdorskaya and incomplete skull VSEGEI 7/2932 from Sengiley [Titov 2008]). The species has been reported from a number of middle and upper Pleistocene sites, mostly in Russia, but remains incompletely described. It differs from extant forms mainly in its larger size and a broad infraorbital shelf.

3. *C. thomasi* Pomel, 1893, from the late early Pleistocene of Tighennif (=Ternifine), housed in MNHN, complemented by photos of the specimens (including the type) kept in the Algiers Museum, kindly provided by Y. Chaïd-Saoudi. The species was first erected for some dental and postcranial remains, but C. Arambourg collected more material from the type locality in 1954-1956, including a complete cranium. This material has been fully described (Martini and Geraads 2018). A few other specimens of *C. thomasi* are from the 'Grotte des Rhinocéros' in Casablanca (Geraads and Bernoussi 2016), but most reports from later sites in North Africa and the Middle East are incorrect (Martini and Geraads 2018). The species is characterized by its large size, pachyostosis (especially marked in the mandible), marked sexual dimorphism, V-shaped choanae, anteriorly located palatine foramina, low placement of orbits, jugular process positioned far from the condyles, an anteriorly positioned P1, P3 with a complete lingual crescent, broad molars with strong styles, an absent or anteriorly located p1, long p4, with a long metaconid, and long limb bones.

4. Early African Camelidae from the early Pliocene of Kossom Bougoudi in Chad (a mandible and two metatarsals housed in Centre National de la Recherche pour le Développement, N'Djamena, Chad (CNRD), described as *Paracamelus gigas* Schlosser, 1903 [Likius et al. 2003] characterized by large size and the presence of a p3); Pliocene of Ichkeul in Tunisia (a calcaneum housed in MNHN [Arambourg 1979; Harris et al. 2010]), Pliocene of Wadi Natrun in Egypt (a cuboid housed in Senckenberg Museum, Frankfurt [Stromer 1902]), Plio-Pleistocene of Turkana Basin of Kenya and Ethiopia (various fragmentary specimens housed in Nairobi National Museum [KNM] and NME [Harris et al. 2010; Howell et al. 1969; Harris 1991; Geraads 2014]), late Pleistocene of Algeria (some isolated teeth housed in Université Claude Bernard, Lyon [UCBL; Flamand 1902]).
5. North American camels housed in the AMNH: *Megacamelus merriami* (Frick, 1921) from Keams Canyon, Arizona, and Edson Quarry, Kansas; *Megatylopus gigas* (Matthew and Cook, 1909) from the Snake Creek Formation of Nebraska; *Megatylopus* sp. from the Guymon area of Oklahoma, and *Aepycamelus major* (Leidy, 1886) from the Mixson beds of Florida. However, because more than one taxon may be present in each of these sites (Harrison 1985), these identifications are not always certain.

Other species are known to us through the literature. The name *Camelus alutensis* was erected (Ştefănescu 1895) for a small mandible from Romania with a p3, a long symphysis, and a shallow corpus, of which we have seen a cast. The species was later transferred to *Paracamelus* (Khaveson 1954). The name *Camelus kujalnensis* Khomenko, 1912, is probably a synonym (Titov 2003), and *Paracamelus minor* Logvynenko, 2001, could be identical as well. This species has also been tentatively reported from the lowermost Pleistocene of Sarikol Tepe in Turkey (Kostopoulos and Sen 1999), but remains poorly known and poorly defined (Ştefănescu 1910; Topachevskiy 1956; Baigusheva 1971; Rădulescu and Burlacu 1993; Logvynenko 2000; Titov 2003). Taxonomy of these small forms is debatable, but the upper molars from Turkey are unlike those of other Camelidae in their U-shaped valleys, and this small-bodied lineage is probably distinct from other forms.

The genus *Paracamelus* was erected for *P. gigas* from the late Neogene of China (Schlosser 1903); it is based upon two upper molars, of which one was selected (Van der Made and Morales 1999) as lectotype; unfortunately, this tooth is no longer part of Schlosser's collection in München (G. Rössner pers. comm.). From the figure (Schlosser 1903: pl. 9, figs. 14 and 26), this molar differs from those of *Camelus* in that both the mesostyle and the buccal pillar of the paracone are distinctly broader, especially near the base, the central anterior valley is wider, and the labial crescents have a less regular thickness. Taken together, these features give the tooth a distinct overall pattern, even suggesting that it might not be camelid at all, but much less scrappy camelid material from Loc. 102 in Henan, China, was assigned to *P. gigas* by Zdansky (1926) so that his material became the reference for this taxon, although species identification was merely based upon size; for the sake of nomenclatural stability, we shall continue using Schlosser's name. Additional material comes from Shansi (Teilhard de Chardin and Trassaert 1937). The species was identified (Teilhard de Chardin and Piveteau 1930) from the early Pleistocene of Nihowan on the basis of absence of a medioplantar astragalar facet on the calcaneus, but this facet may also be lacking in *C. bactrianus* and *C. thomasi* so this identification is unsupported.

The name *Paracamelus alexejevi* Khaveson, 1950, was erected for the abundant material of the Odessa catacombs; later its author (Khaveson 1954) revised Old World camels and provided the first diagnosis of *Paracamelus*, as then understood. It included: 1) presence of p3 and dp2; 2) strong ribs and styles on molars; 3) long P3; 4) paraconid distinct from parastylid on p4; 5) cranium longer and narrower than in *Camelus*, and 6) some differences in mandibular proportions, especially a longer lower jaw. In fact, the morphology that he described and illustrated for the p4 of *P. alexejevi* may be present in *C. dromedarius* as well, although he correctly observed that this species differs from *C. bactrianus* in that the central valley is never closed lingually. The long P3 and presence of p3 are clear, and the long mandible is probably also a valid difference, but other differences in cranial and mandibular proportions remain to be fully documented because the most complete illustrated skull (Khaveson 1954: pls 2 and 10) is largely reconstructed in plaster; in a more reliable cranium (Khaveson 1954: fig. 1), the position of the orbit is similar to that of *Camelus*. The species *P. alexejevi* was defined (Khaveson 1954) by its slender limbs and by the small difference in the mean lengths of the metacarpal and metatarsal (3 mm), but this value is well within the range of extant forms (Martini et al. 2017, and our observations). We have not seen the Ukrainian and Russian material of *Paracamelus*, but some data and photos were provided by T. Krakhmalnaya and N. Podoplelova, and a cast of the type specimen of *P. alutensis* was examined in UCBL.

In addition, several species of poorly constrained age were erected on scrappy material. These are *Procamelus khersonensis* Pavlow, 1904, based upon a juvenile cranium, *Camelus bessarabiensis* Khomenko, 1912 (Simionescu 1930, 1932), and *Camelus praebactrianus* Orlov, 1927 (Orlov 1929), based upon some postcranial bones.

In the purported *Gigantocamelus* sp. from Ukraine (Svistun 1971), the length of the lower molar series looks overestimated, and the distal metapodial is really large only if it is a metatarsal, as assumed by him, but even smaller than in *C. knoblochi* if it is in fact a metacarpal. In '*Gigantocamelus longipes*' from Kazakhstan (Aubekerova 1974) the measurements of a metacarpal match those of a metatarsal of *P. gigas* (Teilhard de Chardin and Trassaert 1937), and should probably be attributed to this species.

Paracamelus aguirrei Morales in Van der Made and Morales, 1999 (this species was first described in an unpublished thesis [Morales 1984]; it seems that the name was validated only in 1999) from Venta del Moro (Morales et al. 1980; Morales 1984; Pickford et al. 1995; Van der Made and Morales 1999) and Librilla (Alberdi et al. 1981) is the earliest camel of Europe, of latest Miocene age. It is poorly known but the upper molars are distinctly brachydont, broad, and have strong styles. A juvenile lower dentition from the upper Miocene of Çoban Pinar, Turkey, was assigned to *Paracamelus* cf. *P. aguirrei* (Van de Made et al. 2002); its provenance remains uncertain (Sen 2010; Van der Made and Morales 2013) but the long, high-crowned m1 matches extant forms. The few postcranials from the middle (?) Pliocene of Garaet Ichkeul in Tunisia (Arambourg 1979) were also assigned to *P. aguirrei* (Van der Made and Morales 1999), with poor support. The same species was reported (Titov and Logvynenko 2006) from the northern shore of the Black Sea in sites assumed to be earlier in age than Venta del Moro and Çoban Pinar.

Probably the most interesting sites for the history of Old World camels are those recently excavated in Syria by the University of Basel. No details have been published yet, but various sites ranging from the early to the late Pleistocene have provided as many as three different species, two of them being giant forms (Martini et al. 2015). It is likely that the very incomplete remains from Latamne (Hooijer 1961) and Ubeidiyeh (Haas 1966; Geraads 1986) will have to be referred to one or more of them.

Description and comparisons

Mille-Logya material:

The specimen NME-MLP-1346 consists of several parts, including some teeth and fragments recovered by screening, but due to their close physical proximity and identical preservation there is no doubt that they all belong to the same individual (Figs. 1-2; Supplementary Information 1). The largest piece is the posterior part of a cranium with parts of the orbits; in addition, there are the left and right maxillae with most of the teeth, parts of the left and right zygomatic bones, and a piece of the snout consisting of partial palate, vertical part of the maxilla, and partial premaxilla. The cranium is dorsoventrally crushed but distortion affected mostly the braincase itself, while the occiput looks virtually undistorted; in addition, the left squamosal is rotated counterclockwise by about 70°, so that the zygomatic arch is now directed almost ventrally. Dental dimensions suggest that this specimen was a young adult female; the great width of the molars compared to their length, the narrow fourth upper premolar, and the strong labial styles match the type specimen of *C. grattardi*.

The only measurement that can be taken accurately, width across occipital condyles, is within the range of extant *Camelus*, although close to its upper limit. Postorbital width is above the extant range, but may have slightly increased because of deformation. Thus, on the whole it is comparable in size to *C. bactrianus*, *C. thomasi*, and *C. sivalensis*, but smaller than *C. knoblochi*.

The snout fragment comprises parts of the palate, the ascending part of the maxilla, and the premaxilla. The last is distinctly narrower than in *C. thomasi* (Martini and Geraads 2018); it certainly did not widen posteriorly, in contrast to that of *C. sivalensis* (AMNH-FM19832) and of most extant specimens, and it is very unlikely that it reached the nasals. The erupting permanent canine is preserved within the bone; its tip just reaches the palatal level; the relatively small size of this tooth, reflected in the lack of lateral inflation of the maxilla, suggests that the cranium is from a female individual. In front of the canine, the alveolus of the missing (shed ?) deciduous canine is visible. Not far behind, about one half of a large P1 alveolus is preserved; it is usually located more posteriorly in *C. bactrianus* (Martini et al. 2017). This (missing) tooth was not much smaller than the canine, confirming the sex of the animal. The P1 may be absent in extant forms and in *C. knoblochi*; it is absent in the one known specimen of *P. gigas*, but given the documented variation in *Camelus*, this is insufficient to bar this species from the ancestry of *Camelus* (contra Zdansky 1926). At the level of the canine, the maxilla reaches the sagittal plane whereas in extant forms the posterior processes of the premaxillae intervene; this suggests that the incisive fissures were located more rostrally in the fossil form. In front of the cheek-teeth, there is no evidence of a crest bordering the palate, nor of a sharp narrowing of the latter anterior to P3. The missing palatine bone reached the limit M1/M2, a position that is within the range of variation of the extant forms. There is a single pair of palatine foramina at the level of the first lobe of M1, a position more common in *C. bactrianus* than in *C. dromedarius*; they are even more posterior in *C. knoblochi*, but in *C. sivalensis* and *C. thomasi*, the main pair of foramina opens at the level of P4, as in most *C. dromedarius*. The choanae are not preserved, but the lateral palatine notches do not reach beyond the posterior border of M3.

The zygomatic bone is almost intact on the left but only a piece of the right bone is preserved; they can be satisfactorily oriented. Posteriorly, the deep groove for the squamosal reaches farther anteriorly, by at least 1 cm, than the level of the posterior border of the orbit. In contrast, in all extant specimens, in *C. knoblochi*, *C. thomasi*, and *P. gigas*, the most rostral point of the squamosal remains distinctly more caudal. The only species showing a squamosal reaching the orbital level is *P. alexejevi* (Khaveson 1954: fig. 1), and the same condition is also observed in *Megacamelus merriami*. Under the orbit, the zygomatic bone forms a flat shelf, about 2 cm deep, facing laterally more than ventrally. It is limited by a clear ventral edge and proceeds posteriorly into the lateral face of the zygomatic arch, whose ventral edge is concave at this level. The maxilla shows that this shelf extends forwards as far as the anterior orbital border and forms a flange over a well-marked longitudinal groove. This shelf is weak in the dromedary, but moderate or variable in other *Camelus*, except in the three specimens of *C. knoblochi*, where it is broad. The small infraorbital foramen is located above P4, as in other Old World camels.

The braincase is rounded and clearly limited anteriorly at the level of the postorbital constriction, but also posteriorly where it is distinctly pinched before the nuchal crest; it may be that deformation increased its greatest width which is located at mid-height. The strong, prominent sagittal crest extends from the nuchal crest to the middle of the braincase, where it gently diverges into the temporal lines. There is a single supraorbital foramen on either side, and they are located far apart (66 mm between their centers). In extant *Camelus*, and in *C. knoblochi*, there are usually multiple foramina, and they are always closer to the midline (Supplementary Information 2–3). The condition in *C. sivalensis* is observable in NHMUK-PV-OR36664: it is similar to that of NME-MLP-1346, with a distance of 64 mm between the centers; the cranium A/646 (Sahni and Khan 1988) has multiple foramina but they are also located rather far apart (photos provided by R. Patnaik).

The mandibular fossa is virtually flat. It is bordered posterolaterally by a postglenoid process, but there is no lateral tubercle on the ventral border of the zygomatic arch. This paraglenoid tubercle is always present in all other species of *Camelus*.

There is no evidence of transverse deformation of the auditory region, cranial base, and occipital, at least on the right side and, save for the left squamosal that is rotated, this area is symmetrical, and distortion is probably minimal. The braincase is somewhat crushed dorsoventrally and it may be that some transverse compressing occurred behind it. The imperfectly preserved right auditory region displays a relatively large tympanic bulla, with inflation anteromedially of the tympanohyal vagina. The basioccipital is strongly pinched in front of the occipital condyles, forming large, deep depressions between the midline and the bullae, as in *C. sivalensis* (NHMUK-PV-OR39597, AMNH-FM19785). Although this is hard to quantify, the basicranium looks short; in contrast, the *C. sivalensis* cranium AMNH-FM19785 looks long, but its central part is incorrectly reconstructed in plaster. The plane of the incomplete jugular process is inclined at more than 45° to the sagittal plane, thus slightly more transversally than in extant forms, *C. knoblochi*, and *C. sivalensis* (NHMUK-PV-OR39597, A/646), and distinctly more so than in *C. thomasi*, in which it is located far away from the occipital condyle. The hypoglossar foramen is not visible.

The central part of the occipital surface, above the foramen magnum, forms a broad pillar that is much more prominent caudally than the lateral parts of the occipital, above the condyles. However, the dorsal part of this raised area is depressed on either side of a weak occipital crest, below the central part of the nuchal crest. Laterally, the nuchal crest is perhaps slightly damaged, but the outline of the occipital was clearly bell-shaped, even accounting for slight transverse crushing. In extant forms, the shape of the occipital mainly depends on the development and degree of flaring of the nuchal crest, but it never looks so narrow; *C. sivalensis* (NHMUK-PV-OR39597; AMNH-FM19785; A/646) and *C. thomasi* (Martini and Geraads 2018) also have broad occipitals.

All cheek-teeth are preserved, either on the right or left sides (Fig. 1; Table 1; Supplementary Information 1). The P3 consists mostly of a buccal crescent, with parastyle, metastyle, and a rounded pillar located slightly mesially, about as prominent as the styles. A crest descends from the distal part of the buccal wall towards the lingual side, and curves mesially to meet a low ridge best indicated mesiolingually and distally, at the base of the main buccal wall. Although this ridge is clearly homologous with a lingual crescent, it clearly remains below occlusal level until late wear. There is much variation in size and morphology of the P3 of Old World camels. In extant forms the lingual crescent is rarely almost complete; it is usually mostly restricted to its distal part, and may be as weak as in NME-MLP-1346. *Camelus knoblochi* also has an incomplete lingual crescent, like

P. gigas (Zdansky 1926). In *C. sivalensis*, instead, all three P3s (NHMUK-PV-M100160, NHMUK-PV-XX40570, AMNH-FM19832) have a fully-formed lingual crescent, and this also seems to be true of other specimens (Gaur et al. 1984; cranium A/646). The single known P3 of *C. thomasi* (Martini and Geraads 2018) also has a complete lingual crescent.

The P4 is still unworn, while M3 is slightly affected by wear. The reverse occurs usually, but not always, in extant forms; the sequence of tooth eruption further differs from that of the extant forms in that all molars are touched by wear before the full eruption of the canine. The buccal crescent of P4 is very similar to that of P3 but, in addition, there is a fully formed lingual crescent that sends a strong distal spur into the central valley; such a spur is smaller or absent in extant *Camelus*, *C. thomasi*, and *C. sivalensis*. Still, this tooth remains long and narrow.

The molars have a faint metacone rib and a more distinct paracone rib. The parastyle and mesostyle are strong, and distinctly overlap the preceding lobe (paracone, or metacone of the preceding tooth); in these strong styles, NME-MLP-1346 resembles more *C. thomasi* and *C. sivalensis* than the average condition of the extant species. Although measurements must be used with caution because length of the molars decreases dramatically with wear, the upper molars are broad relative to their length. This is also true of fossil *Camelus* in general (Supplementary Information 2).

All teeth are rather brachydont, although they possess some cementum cover. Although height cannot be precisely measured on the molars, the height of M3 was certainly less than its length. The unworn P3 is only slightly taller than long, and P4 is only moderately hypsodont. This contrasts with extant *Camelus*, and with the fossil *C. sivalensis* and *C. thomasi* (Table 2). In labial view (Fig. 1F), cusp shape is high and sharp on the little-worn M3s, but more rounded on the M1s (and on isolated, more worn teeth), suggesting a basically browsing behavior.

NME-MLP-2680 best matches the morphology of a lower canine, and is probably from a female individual, and probably of the same individual as NME-MLP-2665 and NME-MLP-2684, two upper molars; the metacone wall is flat, but the mesostyle and paracone rib are better indicated than in extant forms (Fig. 3A–B), and these teeth are broad relative to their length.

Most measurements of the distal tibia NME-MLP-2584 (Fig. 3C) are above the maximum recorded ones for extant *Camelus* (Martini et al. 2017), but the proportions are similar. As in *C. sivalensis*, the medial malleolus is weaker than in extant forms, *C. thomasi*, and *C. knoblochi*, but this feature is variable in North American forms. As for the cranial remains, the large size of the tibia suggests an animal somewhat taller than the living forms, but probably not heavier than well-fed domestic animals, which can reach about 1000 kg.

NME-MLP-1189 is a complete astragalus (Fig. 3D), and NME-MLP-1144 a distal half; the extant forms display a great intraspecific variation but some differences can be observed (Steiger 1990; Martini et al. 2017). NME-MLP-1189 is not broader than other *Camelus*, but taller (Supplementary Information 2–3). The part of distal trochlea that corresponds to the cuboid is narrower than in all *C. dromedarius,* and more like *C. bactrianus*, *C. sivalensis*, and *C. thomasi*, but this cuboid facet is broader in NME-MLP-1144, as in *C. dromedarius*. In lateral view, the tibial facet is strongly convex and its proximal end extends far towards the plantar side (see also Steiger 1990: fig. 52) as being a characteristic of *C. dromedarius* compared to *C. bactrianus*, but also found in *C. sivalensis*, whereas *C. thomasi* resembles more *C. bactrianus*. The lateral calcaneal facet is not contiguous with the plantar one, in contrast to the usual condition in extant forms. Obviously, fossil forms display a mixture of the characters of both extant species, and it would be misleading to search for the extant types of astragali among them, but NME-MLP-1189 is unlike all other species in its slenderness.

Additional material of *Camelus grattardi* from Omo:

The type specimen of *C. grattardi* is from Member G of the Shungura Formation at Omo, Ethiopia (Geraads 2014); these deposits are somewhat younger than all localities in the MLP area. It clearly differs from both extant species in its narrow P4 and broad molars; these characters match those observed in the MLP camel and, given the geographic and chronological proximity, we confidently assign the MLP camel to *C. grattardi*. Thus, features observable on the material from the MLP area can be complemented by those of other specimens of *C. grattardi*. Only some of those from the Omo Shungura Formation have been published (Howell et al. 1969; Grattard et al. 1976; Geraads 2014; Rowan et al. 2018), but we have now been able to examine all specimens from the early expeditions; they are briefly described below.

NME-L480-7 from lower Member G is a piece of mandible with heavily cracked, incomplete m1−m3 (Fig. 4A). At ca. 2.2 Ma, it is the earliest specimen demonstrating the absence of p3. All three molars display an incipient goat fold; although they are worn and damaged, they are relatively high-crowned. The unnumbered lower molar collected by Arambourg in 1933 (Fig. 4C), probably from a similar level, also bears a weak goat fold. This is also true of the m3 in the mandible fragment NME-Omo28-67-494 (upper Member B; Fig. 4D), which has a narrow corpus (thickness at m1−m2 = 33 mm) that is even less thick than that of *C. bactrianus*, but this specimen is older than those formally identifiable as *C. grattardi*.

The color and weathering of the proximal humerus NME-L1-68-36 from Omo Shungura Upper Member B differ from those of the *Camelus* distal humerus NME-L1-68-76, so that there is no evidence that they are from the same individual, in contrast to what was hypothesized (Geraads 2014). Its identification is not straightforward; it was compared with modern *Camelus* (Grattard et al. 1976) but the tuberculum minus is much lower, the tuberculum majus higher, and the medial part of the intertubercular sulcus (bicipital groove) narrower and deeper; it differs in the same features from North American giant camels, and we conclude that NME-L1-68-36 probably belongs to *Giraffa* Brisson, 1772, instead, although not a perfect match with this genus. The distal humerus NME-L1-68-76 is definitely camelid but, at ca. 3 Ma, it is older than other specimens of *C. grattardi*, and it now seems safer not to include it in the hypodigm of the species.

The proximal phalanges NME-Omo 28-67-577 (Upper Member B; Fig. 4E) and NME-Omo 119-68-14 (Member D; Fig. 4B) were, probably correctly, assigned to the anterior and posterior limbs, respectively (Grattard et al. 1976). Both phalanges have relatively shorter distal condyles, and shorter ligament insertions on the palmar/plantar face than in extant *Camelus*. However, whereas in extant forms the posterior proximal phalanx is basically a smaller version of the anterior one, these two Omo phalanges differ little in length, but strongly so in their morphology, NME-Omo 119-68-14 being almost as long as NME-Omo 28-67-577 but distinctly more slender. The former can probably be identified as *C. grattardi*; it differs from extant *Camelus* in its very deep (antero-posteriorly) proximal articulation. The latter can hardly be assigned to the same species and, like other specimens from Shungura Upper Member B, we prefer to leave it as *?Camelus* sp.

Systematic paleontology

CAMELIDAE Gray, 1821

CAMELUS Linnaeus, 1758

Type species—*Camelus bactrianus* Linnaeus, 1758.

CAMELUS GRATTARDI Geraads, 2014

Holotype–NME-Omo75S-70-956, maxilla fragment with P4−M3; from lower Member G (G4 to G13), Shungura Formation, lower Omo valley, Ethiopia; ca. 2.2 Ma.; housed in NME.

Referred material from Mille-Logya–NME-MLP-1346, incomplete cranium including the braincase, parts of the orbits, palate, maxilla, and most of the tooth-rows, found in 2014 by Moges Mekonnen (geographic coordinates 11.56437° N, 40.83878° E); NME-MLP-2680, lower canine; NME-MLP-2665, upper molar; NME-MLP-2684, incomplete upper molar, probably M3; NME-MLP-1189, astragalus; NME-MLP-1144, incomplete astragalus; NME-MLP-2584, distal tibia. All this material is from the Seraitu unit, ca. 2.9 – 2.5 Ma.

Diagnosis–A large member of *Camelus*, with supraorbital foramina located wide apart, squamosal reaching the orbital level, narrow occiput, mesial border of the mandibular ramus strongly inclined backwards, upper molars only slightly longer than broad, with prominent styles, P4 much narrower than M1, proximal phalanges with short posterior scars, posterior proximal phalanx with a deep proximal articulation. Differs from species of *Paracamelus* in the deeper infraorbital shelf, loss of p3, smaller P3, weaker molar ribs, and shorter scars on the proximal phalanges. Differs from all other species of *Camelus* in: tall occiput, squamosal reaching the orbital level, absence of paraglenoid tubercle, deeper mandibular corpus, narrow P4, less hypsodont teeth, and tall astragalus. Differs additionally: from extant *C. bactrianus* and *C. dromedarius* in its late canine eruption, deep infraorbital shelf, supraorbital foraminae wide apart, more oblique anterior border of mandibular ramus, broader molars, stronger, thicker styles in the upper teeth, more cylindrical and more transverse distal humeral articulation, and proximal phalanges with shorter ligament scars; from the Pleistocene North-African *C. thomasi* in its deep infraorbital shelf, supraorbital foraminae wide apart, much less complete P3 lingual crescent, lack of pachyostosis, longer lateral lip and broader cuboid trochlea on the astragalus, and shorter scars on the proximal phalanges; from *C. sivalensis* from the Siwaliks in the deeper infraorbital shelf, less complete P3 lingual crescent, and weaker molar ribs.

Parsimony analysis

Old World fossil camels have to date been mostly represented by incomplete remains. Most previous studies assumed, a priori, that they were more closely related to one or the other of the extant forms than to other stem camelids. The new finds from the MLP area, in conjunction with the recent reappraisal of the distinguishing features between the extant taxa (Martini et al. 2017), the study of the only other significant African sample (Martini and Geraads 2018), and the revision of incompletely described samples allow for a comprehensive analysis of their relationships (Supplementary Information 2 and 4). A total of 22 characters, all ordered (Supplementary Information 2–4), were used in a parsimony analysis, using TNT (Goloboff et al. 2003; Goloboff and Catalano 2016) and PAUP*4 (Swofford 2003). To the *Camelus* species mentioned above, we added *P. gigas*, *P. alexejevi*, and *P. alutensis*. Because Old World camels immigrated from North America, the outgroup taxon must be sought there. We chose *Megacamelus merriami*, which is the best-documented close relative of Old World camels.

Our parsimony analysis yields three equally parsimonious trees that differ only in the branching pattern within *Paracamelus* (the resolution of this trichotomy with the highest bootstrap frequency is shown in Fig. 5). The trees indicate that *Camelus grattardi* is the most basal branch of the *Camelus* clade. It is followed by the southern Asian *C. sivalensis*, and the North Africa *C. thomasi*; this succession is consistent with the ages of these species, *C. sivalensis* being of early Pleistocene age, *C. thomasi* of late early to early middle Pleistocene age. The newly recovered MLP material provides the oldest evidence (at 2.9 – 2.5 Ma) of one of the most diagnostic characters for the species, a small P3. By contrast, on the mandible KNM-ER 2608 from the Koobi Fora Formation dated to ca. 3.5 Ma (Harris 1991), the absence of p3, functionally correlated with a small P3, cannot be definitely ascertained, and the predental portion is extremely long, suggesting that KNM-ER 2608 potentially documents instead one the latest occurrences of *Paracamelus* in Africa. *Camelus grattardi* thus suggests that the genus *Camelus* arose in eastern Africa ca. 3 Ma, when *Paracamelus* went extinct.

The precise dating of *C. grattardi* has important consequences on the chronology of the origin and diversification of the genus *Camelus*. The results of the parsimony analysis are consistent with the chronology of the fossil record. Our results are only moderately robust, but the most robust clade is precisely that which includes only crown camelids, with a bootstrap of 70% and a decay index (Bremer 1988) of 2. Our estimate of the minimal age for the crown group, for the divergence between *C. dromedarius* and *C. bactrianus*, is about 0.6 to 0.8 Ma and matches the age of the oldest known remains of *C. knoblochi* (Titov 2008), No fossil form that could be part of this crown clade is known before the middle Pleistocene, so there is no fossil evidence that this crown clade predates the middle Pleistocene. In fact, even this age could be too old, as it rests upon the poorly known *C. knoblochi* (Titov 2008); should detailed study of this species show that it is in fact no more closely related to *C. dromedarius* than to *C. bactrianus*, a possibility raised by the low Bremer index (1) and low bootstrap frequency (50%) of the node uniting *C. knoblochi* to *C. dromedarius*, the divergence between the extant taxa could even be younger. The position of *C. knoblochi* in the crown of *Camelus* dispels doubts that the topology of crown *Camelus* is influenced by domestication because if the latter had caused considerable phenotypic convergence between *C. dromedarius* and *C. bactrianus*, the long extinct (hence, undomesticated) *C. knoblochi* should logically be excluded from the crown.

Conclusion

Our estimate of the minimal divergence date between the lineages leading to the extant species, certainly not earlier than the middle Pleistocene and perhaps late in this age, is much more recent than the estimates provided by molecular analyses: ca. 4.4 Ma using the whole genome (Wu et al. 2014), and ca. 4.1 Ma by comparison with the genome of the late middle Pleistocene American *Camelops* Leidy, 1854 (Heintzmann et al. 2015). On the basis of the mtDNA sequence, it was even suggested (Cui et al. 2007) that this divergence occurred before the Camelidae immigrated into the Old World, ca. 8 Ma.

Our analysis based on morphological and stratigraphic data suggests *Camelus* dates from the late Pliocene, and the divergence of the extant lineages is much younger than estimated by molecular analyses. Of course, part of the discrepancy may reflect the fact that paleontological data directly provide only minimal divergence age estimates, whereas molecular ages attempt to provide unbiased estimates of divergence dates, but this factor alone is unlikely to account for the five-fold difference or more between our paleontological estimate and molecular estimates. A number of increasingly sophisticated and realistic methods have been developed to get unbiased estimates and confidence intervals from paleontological data (e.g., Strauss and Sadler 1989; Marshall 2008), but this requires extensive dataset compilation and the use of methods that are beyond the scope of our study. Nevertheless, our estimate is also supported by the fertility of *C. dromedarius* × *C. bactrianus*, whose hybrids are fertile up to the F4 when backcrossed with either species (Faye and Konuspayeva 2012). Among other artiodactyls, fertile hybrids are unknown between species whose divergence is earlier than the Pleistocene (Gray 1972).

Extant *Camelus* developed a number of physiologic adaptations to life in subdesertic conditions (Wu et al. 2014). By contrast, stem *Camelus* seem to be associated with a variety of fossil assemblages, and might have been able to thrive in diverse environments, but none of them is suggestive of subdesertic conditions. Pending detailed analysis of the ecology of fossil Old World camels, the adaptation to desert conditions may be another, recently acquired synapomorphy of extant *Camelus*.

Acknowledgments

We thank the Authority for Research and Conservation of Cultural Heritage and the Afar Regional State for permission to conduct field work in the Mille-Logya area. We also express our gratitude to the people of the Mille and Logya towns and environs for permission and logistical support. We are grateful to C. Argot and J. Lesur (MNHN), G. Baryshnikov (ZIN), D. Berthet (CCEC), P. Brewer (NHMUK), J. Galkin (AMNH), T. Getachew and Y. Assefa (NME), M. Muungu (KNM), and E. Robert (UCBL) for access to collections, to J.-P. Brugal, Y. Chaïd-Saoudi, B. Kear, T. Krakhmalnaya, P. Martini, J. Morales, R. Patnaik, N. Podoplelova, G. Rössner, and V. Titov for photos and other data on fossil collections, to P. Loubry for the photos of Fig. 4, to V. Codrea, P. Martini, and N. Spassov for their help with foreign literature, and to S. Colombero and J. Rowan, whose comments significantly improved the manuscript. Funding to conduct field work was provided by Margaret and Will Hearst.

Supplementary Information:

Supplementary Information 1. 3D reconstruction of NME-MLP-1346 (made with Agisoft Photoscan). [File Geraads&al_Camelus_SupInfo1.pdf]

Supplementary Information 2. Description of the characters used in the parsimony analysis; matrix and character list, in TNT format. [File Geraads&al_Camelus_SupInfo2.docx]

Supplementary Information 3. Raw measurements used in Supplementary Information 1 [File Geraads&al_Camelus_SupInfo3.xlsx]

Supplementary Information 4. Matrix used in the parsimony analysis, in Nexus format. [File Geraads&al_Camelus_SupInfo4.nex]

References

Alberdi MT, Morales J, Moya S, Sanchiz B (1981) Macrovertebrados (Reptilia y Mammalia) del yacimiento finimioceno de Librilla (Murcia). Estud geol 37: 307–312

Alemseged Z, Barr WA, Bobe R, Geraads D, McPherron S, Reed D, Wynn J (2016) A new late Pliocene Fauna from the Mille-Logya Project (MLP) Area, Afar Regional State, Ethiopia. 24th Annual Meeting of the Paleoanthropology Society, Atlanta, GA

Arambourg C (1979) Vertébrés villafranchiens d'Afrique du Nord (artiodactyles, carnivores, primates, reptiles, oiseaux). Fondation Singer-Polignac, Paris, 141 pp

Aubekerova PA (1974) New giant camel from Pliocene deposits of Tekess depression. Materials for the history of fauna and flora of Kakakhstan, Akad Nauk SSR Kazhakstan Inst Zool 6: 74−82 [in Russian]

Baigusheva VS (1971) Fossil theriofauna of the Liventzovka sand-pit. Tr Zool Inst Akad Nauk 49: 5−29 [in Russian]

Bibi F, Rowan J, Reed K (2017). Late Pliocene Bovidae from Ledi-Geraru (Lower Awash Valley, Ethiopia) and their implications for Afar paleoecology. J Vertebr Paleontol doi:10.1080/02724634.2017.1337639

Boule M, Breuil H, Licent E, Teilhard de Chardin P (1928) Le Paléolithique de la Chine. Arch Inst paléontol hum 4: 1–138

Bremer K (1988) The limits of amino acid sequence data in angiosperm phylogenetic reconstruction. Evolution 42: 795–803

Colbert EH (1935) Siwalik mammals in the American Museum of Natural History. Trans Amer

Philos Soc 26: 1–401

Colombero S, Bonelli E, Pavia M, Repetto G, Carnevale G (2017) *Paracamelus* (Mammalia, Camelidae) remains from the late Messinian of Italy: insights into the last camels of western Europe. Hist Biol 29: 509–518

Cui P, Ji R, Ding F, Qi D, Gao H, Meng H, Yu J, Hu S, Zhang H (2007) A complete mitochondrial genome sequence of the wild two-humped camel (*Camelus bactrianus ferus*): an evolutionary history of Camelidae. BMC genomics 8(241), doi:10.1186/1471-2164-8-241

Falconer H, Cautley PT (1836) Note on the fossil camel of the Siwalik Hills. Asiatic Res 19: 115–134

Falconer H, Cautley PT (1846) Fauna Antiqua Sivalensis, Being the Fossil Zoology of the Sewalik Hills, in the North of India. Smith, Elder and Co, London, 590 pp

Faye B, Konuspayeva G (2012) The encounter between bactrian and dromedary camels in Central Asia. In: Knoll EV, Burger P (eds) Camels in Asia and North Africa: Interdisciplinary Perspectives on Their Past and Present Significance. Österreichische Akademie der Wissenschaften, Wien, pp 27–33

Flamand GBM (1902) Sur l'utilisation, comme instruments néolithiques, de coquilles fossiles à taille intentionnelle (littoral nord-africain). C R Assoc fr Av Sci 30: 729–734

Frick C (1921) Extinct vertebrate faunas of the badlands of Bautista creek and San Timoteo cañon, Southern California. Univ Calif Publ Bull Dept Geol 12: 277–424

Gaur R, Raghavan P, Chopra SRK (1984) On the remains of *Camelus sivalensis* (Artiodactyla, Camelidae) from Pinjor Formation of Upper Sivaliks. Ind J Earth Sci 11: 158–165

Geraads D (2014) *Camelus grattardi* nov. sp., a new camel from the Shungura Formation, Omo valley, Ethiopia, and the relationships of African fossil Camelidae (Mammalia). J Vertebr Paleontol 34: 1481–1485

Geraads D (1986) Ruminants pléistocènes d'Oubeidiyeh. Mém Trav Cent Rech fr Jérus 5: 143–181

Geraads D, Bernoussi R (2016) Hippopotamidae, Suidae et Camelidae. In: Raynal J-P, Mohib A (eds) Préhistoire de Casablanca. 1. La Grotte des Rhinocéros (Fouilles 1991 et 1996). Villes et Sites Archéologiques du Maroc, 6, Ministère de la Culture, INSAP, Rabat, pp 133−134

Goloboff PA, Catalano SA (2016) TNT version 1.5, including a full implementation of phylogenetic morphometrics. Cladistics 32: 221−238

Goloboff PA, Farris J, Nixon K (2003) TNT, Tree analysis using New Technology [software]. www.lillo.org.ar/phylogeny/tnt

Grattard J-L, Howell FC, Coppens Y (1976) Remains of *Camelus* from the Shungura Formation, lower Omo valley. In: Coppens Y, Howell FC, Isaac GLl, Leakey REF (eds) Earliest Man and Environments in the Lake Rudolf Basin. University of Chicago Press, Chicago, pp 268–274

Gray AP (1972) Mammalian hybrids: a check-list with bibliography. Commonwealth Agricultural Bureaux, Slough, 262 pp

Gray JE (1821) On the natural arrangment of vertebrose animals. London Medical Repository 15: 296–310.

Haas G (1966) On the Vertebrate Fauna of the Lower Pleistocene Site 'Ubeidiya. Israel Academy of Sciences and Humanities, Jerusalem, 68 pp

Harris JM (1991) Camelidae. In: Harris JM (ed) Koobi Fora Research Project. Volume 3: The Fossil Ungulates: Geology, Fossil Artiodactyls and Palaeoenvironments. Clarendon Press, Oxford, pp 86–91

Harris JM, Geraads D, Solounias N (2010) Camelidae. In: Werdelin L, Sanders WJ (eds.) Cenozoic Mammals of Africa. University of California Press, Berkeley, pp 815–820

Harrison JA (1985) Giant camels from the Cenozoic of North America. Smithson Contrib Paleobiol 57: 1–29

Heintzman PD, Zazula GD, Cahill JA, Reyes AV, MacPhee RDE, Shapiro B (2015) Genomic data from extinct North American *Camelops* revise camel evolutionary history. Mol Biol Evol 32: 2433–2440

Honey JG, Harrison JA, Prothero DR, Stevens MS (1998) Camelidae. In: Janis CM, Scott KM, Jacobs LL (eds.) Evolution of Tertiary Mammals of North America. Volume 1. Terrestrial Carnivores, Ungulates, and Ungulatelike Mammals. Cambridge University Press, Cambridge, pp 439–462

Hooijer DA (1961) Middle Pleistocene mammals from Latamne, Orontes valley, Syria. Ann archéol Syrie 11: 117−132

Howell FC, Fichter LS, Wolf R (1969) Fossil camels in the Omo beds, southern Ethiopia. Nature 223: 150–152

Khaveson IaI (1954) Camels from the Tertiary of the Oriental hemisphere (genus *Paracamelus*). Trudy paleontol Inst 47: 100–162 [in Russian]

Khaveson IaI (1950) Camels of the genus *Paracamelus*. Dokl Akad Nauk SSSR 70: 917–920 [in Russian]

Khomenko IP (1912) *Camelus bessarabiensis* und andere fossile Formen Süd-Bessarabiens. Travaux de la Société des Naturalistes et des Amateurs des Sciences naturelles de Bessarabie, 3: 92-127 [Russian and German]Kostopoulos DS, Sen S (1999) Late Pliocene (Villafranchian) mammals from Sarikol Tepe, Ankara, Turkey. Mitt Bayer Staatssamml Paläontol hist Geol 39: 165−202

Kozhamkulova BS (1986) The late Cenozoic two-humped (bactrian) camels of Asia. Quartärpaläontol 6: 93−97

Leidy J (1886) Mastodon and llama from Florida. Proc Acad nat Sci Philadelphia 1886: 11−12

Likius A, Brunet M, Geraads D, Vignaud P (2003) Le plus vieux Camelidae (Mammalia, Artiodactyla) d'Afrique: limite Mio-Pliocène, Tchad. Bull Soc géol Fr 174: 187–193

Linnæus C (1758) Systema naturæ per regna tria naturæ, secundum classes, ordines, genera, species, cum characteribus, differentiis, synonymis, locis. Tomus I. Editio decima, reformata. Salvii, Stockholm, 824 pp.

Logvynenko VM (2000) Camels (Camelidae, Tylopoda) from the Pliocene and Pleistocene of

Ukraine. Vestn zool Suppl 14: 120–127 [in Ukrainian]

Logvynenko V (2001) *Paracamelus minor* (Camelidae, Tylopoda) – a new camelid species from the middle Pliocene of Ukraine. Vestn zool 35: 39–42

Martini P, Geraads D (2018) *Camelus thomasi* (Mammalia, Camelidae) from the type-locality Tighennif, Algeria. Geodiversitas 40: 115–134

Martini P, Costeur L, Le Tensorer J-M, Schmid P (2015) Pleistocene camelids from the Syrian desert: the diversity in El Kowm. Anthropologie 119: 687–693

Martini P, Schmid P, Costeur L (2017) Comparative morphometry of the bactrian camel and dromedary. J Mammal Evol 25: 407–425

Marshall CR (2008) A simple method for bracketing absolute divergence times on molecular phylogenies using multiple fossil calibration points. Am Nat 171: 726–742.

Matthew WD, Cook HJ (1909) A Pliocene fauna from western Nebraska. Bull Am Mus Nat Hist 50: 59–210

Morales J (1984) Venta del Moro: su macrofauna de mamíferos, y bioestratigrafía continental del Mioceno terminal Mediterraneo. PhD thesis, Universidad Complutense de Madrid

Morales J, Soria D, Aguirre E (1980) Camélido finimioceno en Venta del Moro, primera cita para Europa Occidental. Estud geol 36: 139–142

Nanda AC (1978) Occurrence of *Camelus sivalensis* Falconer and Cautley from the Tatrot Formation of Ambala, India. J Geol Soc India 19: 160–164

Nehring A (1901) Herr A. Nehring gab eine vorläufige Mittheilung über einen fossilen Kamel-Schädel (Camelus knoblochi) von Sarepta an der Wolga. Sitz-Ber Gesell naturforsch Freunde Berlin 5: 137–144

Orlov YA (1927) Über die Reste eines fossilen Kamels aus dem Gouvernement Akmolinsk (West-Sibirien). Ežegod zool muž 28: 496–538

Orlov YA (1929) Über die Reste der fossilen Cameliden aus dem Gouv. Akmolinsk (Westsibirien). Ežegod zool muž 30: 549–587

Patnaik R (2013) Indian Neogene Siwalik mammalian biostratigraphy. An overview. In: Wang X, Flynn LJ, Fortelius M (eds) Fossil Mammals of Asia: Neogene Biostratigraphy and Chronology. Columbia University Press, New York, pp 423–444

Pavlow M (1904) *Procamelus* du gouvernement de Kherson. Mém Soc Nat nouv Russie 25: 113–133

Pickford M, Morales J, Soria D (1995) Fossil camels from the upper Miocene of Europe: implications for biogeography and faunal change. Geobios 28: 641–650

Pomel A (1893) Paléontologie - Monographies - Caméliens et Cervidés. Carte géologique de l'Algérie, Alger, 50 pp.

Przewalski NM 1878 From Kul'dzha through Tyan'-Shan' to Lob-Nor. St Petersburg, 1878 [in Russian.]

Rădulescu C, Burlacu D (1993) On the presence of *Paracamelus alutensis* (Gr. Ştefănescu) (Camelidae, Mammalia) at Frăteşti (Giurgiu Dept., Romania). An Univ Bucureşti Geol 42: 65–68

Robinson JR, Rowan J, Campisano CJ, Wynn JG, Reed KE (2017) Late Pliocene environmental change during the transition from *Australopithecus* to *Homo.* Nature Ecol Evol 1(159) doi:10.1038/s41559-017-0159

Rowan J, Locke EM, Robinson JR, Campisano CJ, Wynn JG, Reed KE (2016) Fossil Giraffidae (Mammalia, Artiodactyla) from Lee Adoyta, Ledi-Geraru, and late Pliocene dietary evolution in giraffids from the Lower Awash Valley, Ethiopia. J Mammal Evol. doi:10.1007/s10914-016-9343-z

Rowan J, Martini P, Likius A, Merceron G, Boisserie J-R (2018) New Pliocene remains of *Camelus grattardi* (Mammalia, Camelidae) from the Shungura Formation, lower Omo Valley, Ethiopia, and the evolution of African camels. Hist Biol. doi:10.1080/08912963.2017.14234852018

Rybczynski N, Gosse JC, Harington CR, Wogelius RA, Hidy AJ, Buckley M (2013) Mid-Pliocene warm-period deposits in the high arctic yield insight into camel evolution. Nature Comm 4(1550). doi:10.1038/ncomms2516

Sahni MR, Khan E (1988) Pleistocene Vertebrate Fossils and Prehistory of India. Books and Books, New Dehli, 80 pp

Schlosser M (1903) Die fossilen Säugethiere Chinas. Abh k bayer Akad Wiss Math-Phys Kl 22, 1–220

Sen S (2010) Camels do not occur in the late Miocene mammal locality of Çobanpinar, Turkey. Russ J Theriol 9: 87–91

Simionescu I (1930) Les vertébrés pliocènes de Măluşteni (Roumanie). Publ Fond Vasile Adamachi 9: 1–69

Simionescu I (1932) Tertiäre und pleistozäne Camelidae in Rumänien. Bull Sect sci Acad roum 15: 1–8

Ştefãnescu G (1895) Le chameau fossile de Roumanie. Anu Mus Geol Paleontol 1894: 91–123

Ştefãnescu G (1910) Le chameau fossile de Roumanie est l'ancêtre des chameaux dromadaire et du chameau sauvage d'Afrique. Anu Mus Geol Paleontol 4: 48–69

Steiger C (1990) Vergleichend morphologische Untersuchungen an Einzelknochen des postkranialen Skeletts der Altweltkamele. PhD thesis, Tierärztlichen Ludwig-Maximilians Universität, München

Strauss D, Sadler PM (1989) Classical confidence intervals and Bayesian probability estimates for ends of local taxon ranges. Math Geol 21: 411–427.

Stromer E (1902) Wirbeltierreste aus dem mittleren Pliocän des Natrontales und einige subfossile und recente Säugetierreste aus Aegypten. Z dtsch geol Ges 54: 108–115

Svistun VI (1971) New findings of camel (Tylopoda, Camelidae) remains in Pontian deposits of the South of the USSR European part. Vestn zool 1: 64–68 [in Russian]

Swofford DL (2003) PAUP* Phylogenetic Analysis Using Parsimony (*and other methods). Sinauer Associates, Sunderland. Version 4.01 (build 163)

Teilhard de Chardin P, Piveteau J (1930) Les mammifères fossiles de Nihowan, Chine. Ann Paléontol 19: 1–134

Teilhard de Chardin P, Trassaert M (1937) The Pliocene Camelidae, Giraffidae, and Cervidae of south-eastern Shansi. Palaeontol Sin C 1 (102): 1–68

Titov VV (2003) *Paracamelus* from the late Pliocene of the Black Sea region. In: Petculescu A, Ştiucă E (eds) Advances in Vertebrate Paleontology 'Hen to Panta'. Emil Racoviţă Institute of speleology, Bucharest, pp 17–24

Titov VV (2008) Habitat conditions for *Camelus knoblochi* and factors in its extinction. Quaternary Internatl 179: 120–125

Titov VV, Logvynenko V (2006) Early *Paracamelus* (Mammalia, Tylopoda) in Eastern Europe. Acta zool cracov 49A: 163–178

Topachevskiy VA (1956) Remains of small camel (*Paracamelus alutensis*) from the upper Pliocene deposits of the south of Ukraine. Akad Nauk Ukr RSR, Tr Inst Zool 13: 93–100 [in Ukrainian]

Van der Made J, Morales J (1999) Family Camelidae. In: Rössner GE, Heissig K (eds) The Miocene Land Mammals of Europe. Pfeil, München, pp 221–224

Van der Made J, Morales J (2013) Camelids do not occur in the late Miocene mammal locality of Çoban Pinar, Turkey – omissions and contradictions. Russ J Theriol 12: 39–40

Van der Made J, Morales J, Sen S, Aslan F (2002) The first camel from the upper Miocene of Turkey and the dispersal of the camels into the Old World. C R Palevol 1: 117–122

World Association of Veterinary Anatomists (1973) Nomina Anatomica Veterinaria, second ed, A Holzhausen's successors, Vienna, 218 pp

Wu H, Guang X, Al-Fageeh MB, Cao J, Pan S, Zhou H, Zhang L, Abutarboush MH, Xing Y, Xie Z, Alshanqeeti AS, Zhang Y, Yao Q, Al-Shomrani BM, Zhang D, Li J, Manee MM, Yang Z, Yang L, Liu Y, Zhang J, Altammami MA, Wang S, Yu L, Zhang W, Liu S, Ba L, Liu C, Yang X, Meng F, Wang S, Li L, Li E, Li X, Wu K, Zhang S, Wang J, Yin Y, Yang H, Al-

Swailem AM, Wang J (2014) Camelid genomes reveal evolution and adaptation to desert environments. Nature comm 5 (5188): 1–9

Zdansky O (1926) *Paracamelus gigas* Schlosser. Palaeontol Sin C2 (4): 1–44

Figure captions

Figure 1. Main elements of NME-MLP-1346. A: braincase in occipital view; B: braincase in left lateral view; C: braincase in dorsal view; D: left zygomatic arch; E: left upper tooth row with P3–M3, occlusal view; F: same specimen, buccal view. Scale bar, 20 cm for Figs A–C, 10 cm for Figs D–F. See also Supplementary Information 4.

Figure 2. Schematic reconstruction of NME-MLP-1346. Distortion of the temporal and orbital areas prevents accurate reconstruction.

Figure 3. *Camelus grattardi* from Mille-Logya. A: upper left molar NME-MLP-2665. B: incomplete upper right molar NME-MLP-2684. C: distal right tibia NME-MLP-2584. D: left astragalus NME-MLP-1189. Scale bar, 5 cm for Figs A–B, 10 cm for Figs C–D.

Figure 4. Camelidae from the Omo Shungura Formation; A–C: *Camelus grattardi*; D–E: *?Camelus* sp. A: left mandible with m1, m2, incomplete m3, and roots of p4, NME-L480-7, oblique view. B: proximal (posterior ?) phalanx NME-Omo 119-68-14, plantar view. C: right lower molar (probably m2), collected by C. Arambourg, occlusal view. D: right mandible with m3, NME-Omo 28-67-494, occlusal view. E: proximal (anterior ?) phalanx NME-Omo-28-67-577, palmar view. Scale bar, 10 cm.

Figure 5. One of the most parsimonious trees obtained by TNT and PAUP. L = 48; ci = 60; ri = 64. *C.* = *Camelus*; *M.* = *Megacamelus*; *P.* = *Paracamelus*. Extant taxa are in bold. Support values are given as bootstrap / Bremer (decay) index values. Unambiguous synapomorphies are: Node 6: length c–m1 / length m1–m3 (0→1). Node 5: p3 present (0→1); P3 relative to P4 (0→1). Node 4: paraglenoid tubercle (0→1); WP4 / WM1 (0→1). Node 3: mandibular thickening (0→1); scars on proximal phalanges (0→1). Node 2: ramus ascendens (0→1); WP4 / WM1 (1→2); molar

length/breadth (0→1); upper molar styles (0→1). Node 1: choanae (0→1). *Paracamelus alutensis*: size (1→0); mandibular thickening (0→1). *P. gigas*: size (1→2); squamosal reaches orbital level (0→1); metapodials relative to femur (2→1). *C. thomasi*: mandibular thickening (1→2); p4 molarization (1→2). *C. bactrianus*: metapodials relative to femur (0→1). *C. dromedarius*: infraorbital shelf (1→0); mandibular thickening (1→0); p4 molarization (1→0); astragalus cuboid facet (0→2). *C. knoblochi*: size (1→2); infraorbital shelf (1→2); p4 molarization (1→2).

Table captions

Table 1. Dental measurements of NME-MLP-1346 (L = length; W = width).

Table 2. Tooth height in some *Camelus*; height of unworn molars cannot be measured in most specimens, because their base is concealed in bone. Height of unworn teeth is underlined.

SUPPLEMENTARY INFORMATION 2

Character description (their numbers follow those of the data matrix (at the end of this files in TNT format; also in Nexus format as Supplementary Information 4); those that were regarded as too variable, too ambiguous to be used, or autapomorphic, are listed separately and identified by letters. Figures are not to scale; see also figures of the main text for *C. grattardi*.)

0) overall size is rather homogeneous but *Megacamelus*, *P. gigas*, and *C. knoblochi* are larger, whereas *P. alutensis* is smaller.

1) the choanae are V-shaped in most species, but those of *C. dromedarius* are usually more U-shaped (Martini *et al.* 2017); unexpectedly, those of the Razdorskaya skull of *C. knoblochi* (Titov 2008, fig.2) are rather U-shaped.

2) The ventral orbital margin is narrow in *C. dromedarius* and *C. thomasi*, but forms a variably deep shelf in other species.

Character 2, ventral orbital margin. 1) *Megacamelus merriami* (AMNH FM23201), broad; 2) *Camelus dromedarius* (CCEC 5000-2069), narrow; 3) *Camelus knoblochi* (ZIN 8678), broad

3) the squamosal tongue on the zygomatic arch reaches the level of the orbit in *C. grattardi* (Fig. 1 of the main text) and *P. alexejevi* (Khaveson 1954, fig. 1), and comes close to it in *M. merriami*, but is distinctly behind it in other species (not scored in *C. sivalensis* because, although several specimens preserve this area, the sutures are not clearly identifiable).

Character 3, anterior extent of the squamosal tongue 1) *Megacamelus merriami* (AMNH FM23201), almost reaching orbital level 2) modern *Camelus*, behind it.

4) The supra-orbital foramina are close to each other in modern *Camelus* and *M. merriami*, but wider apart in *C. sivalensis* and *C. grattardi*; the condition is unknown in *Paracamelus*.

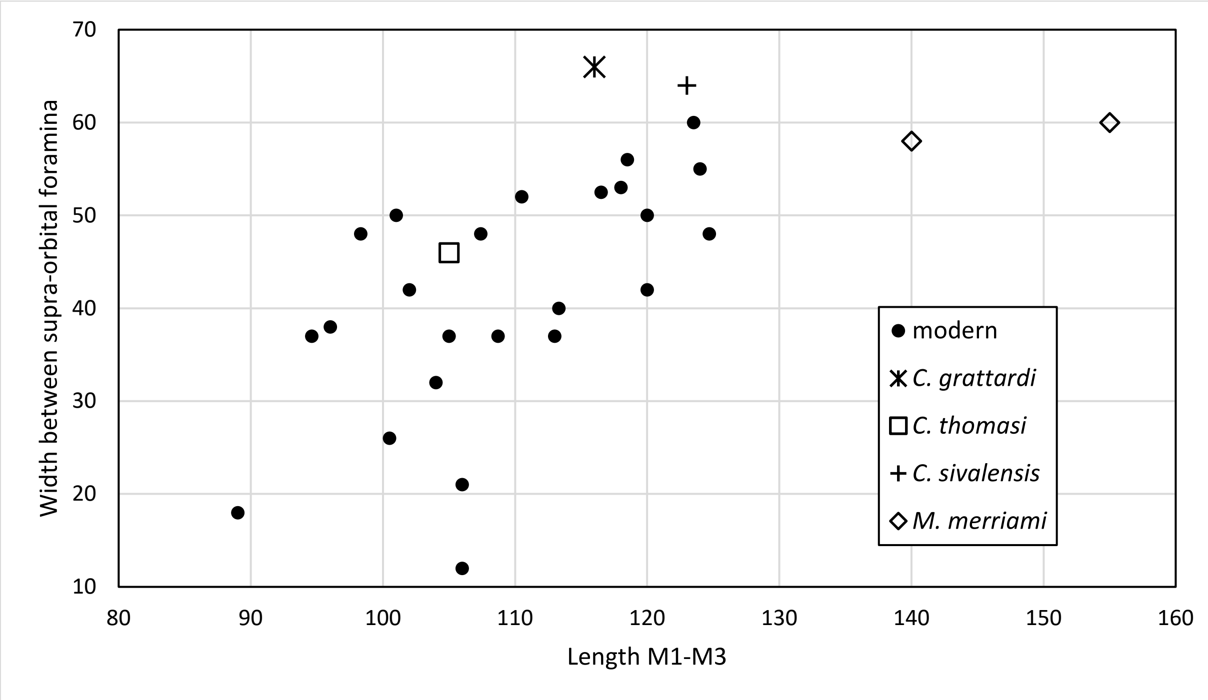

Character 4, distance between the supra-orbital foramina (raw data in Supplementary Information 3)

5) the paraglenoid tubercle, lateral to the glenoid fossa, is present in most *Camelus* but absent in *C. grattardi*, American forms, and at most weak in *Paracamelus* (Zdansky 1926:5 'Der dieselbe bei rezenten Kamelen aussen begrenzende Vorsprung ist kaum vorhanden.'; Khaveson 1954, fig. 1)

Character 5, paraglenoid tubercle. 1) *Megacamelus merriami* (AMNH FM104395), absent; 2) *Camelus bactrianus* (MNHN ZM.1970-44), present.

6) the length of the muzzle can be estimated by the length between the lower canine and m1 (thus obviating for the rare preservation of the incisors and the irregular presence of p3). This measurement separates *Paracamelus*, in which it is distinctly greater than the length m1−m3, from *Camelus* and N. American forms, in which it is at most slightly longer. The shortness of the muzzle in *C. grattardi* is inferred from the juvenile specimen KNM-WT-39366, from just below the Lokalalei tuff at c. 2.55 Ma, in which it is as short as in modern *Camelus* of similar ontogenic age. The incomplete mandible KNM-ER-2608 probably had a longer pre-dental portion, but could belong to *Paracamelus* instead. No measurement can be taken on *C. thomasi*, but MNHN TER-1685 unambiguously shows that the muzzle was short.

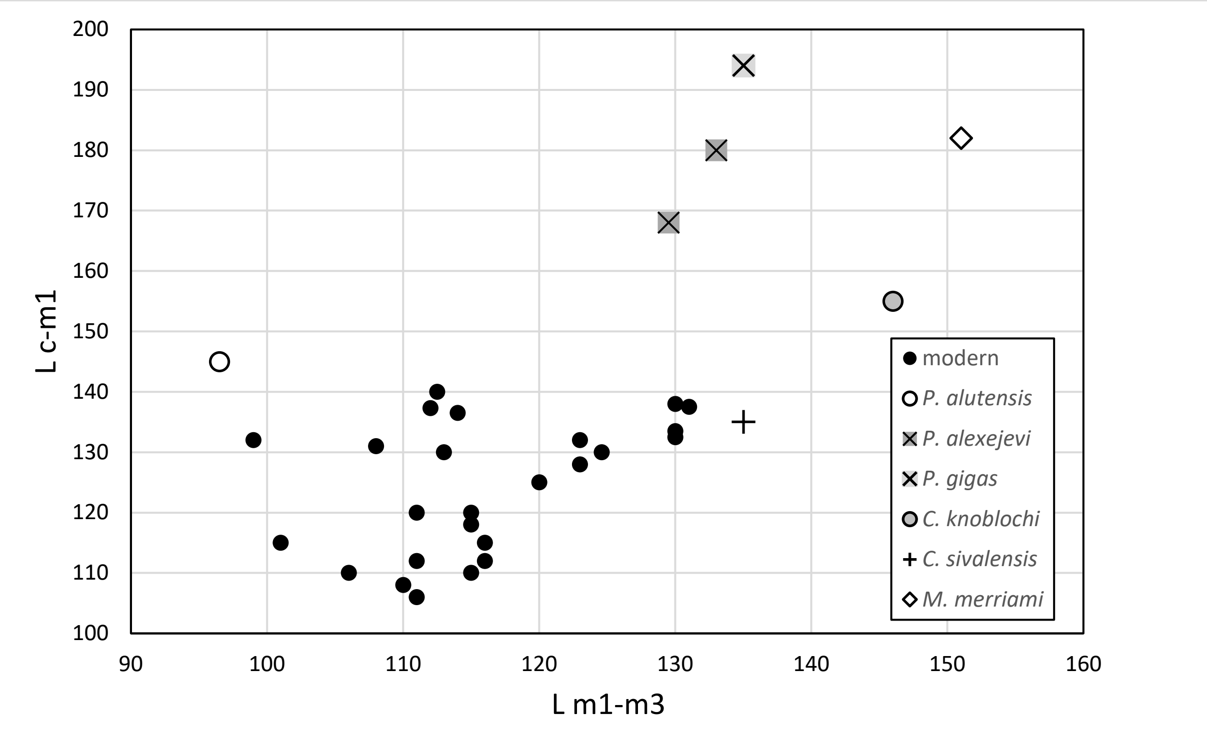

Character 6, relative length of the predental portion of the muzzle, a proxy for the length of the muzzle. The smallest modern *Camelus* is a very old specimen, in which wear has reduced molar length (raw data in Supplementary Information 3).

7) the ascending ramus of the mandible displays significant differences, with limited intra-specific variation (in *Camelus*, the shape of the coronoid process is a good distinguishing feature at species level [Martini *et al.* 2017; Martini & Geraads 2018]). The anterior border of the ramus is usually oblique, but vertical or even slightly inclined forwards in younger forms, but also in *M. merriami*.

Character 7, anterior border of the ascending ramus. 1) *Megacamelus merriami* (AMNH FM23216), vertical; 2) modern *Camelus*, vertical; 3) *Camelus grattardi* (KNM-WT 16454), oblique; 4) *Camelus thomasi*, oblique.

8) all camels have a robust mandibular corpus; although there is much intra-specific variation, this is especially marked in *C. bactrianus*, *C. knoblochi*, and *P. alutensis*, and still more so in *C. thomasi*, whose pachyostosis is highly characteristic.

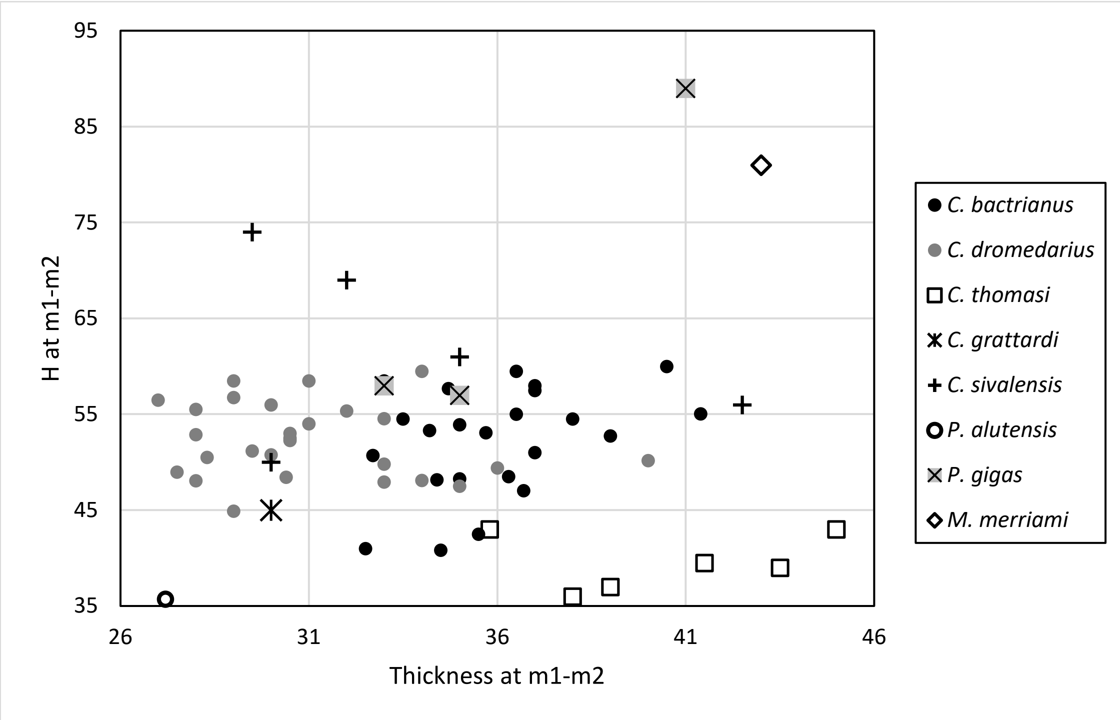

Character 8, plot of mandibular corpus depth vs. thickness between m1 and m2 (raw data in Supplementary Information 3).

9) The loss of p3 is the best diagnostic character of *Camelus*, unambiguously distinguishing it from *Paracamelus* in the Old World. The earliest precisely dated fossil lacking this tooth is the mandible NME-L480-7 from Omo Shungura G3 at c. 2.2 Ma.

10) a shortening of P3 is probably functionally correlated with the loss of p3.

11, 12) It seems that this loss of p3 is associated with a trend towards a greater molarisation of P3 and p4, through the development of a lingual wall. The lingual crescent of P3 is complete in all known specimens of *C. sivalensis* (NHMUK-M 15347, AMNH-FM19832, Gaur et al., 1984, fig.2) and *C. thomasi* (Martini & Geraads 2018). The p4 is variable in *C. sivalensis* and *C. bactrianus*, but on the average it is more molarized in the latter species than in *C. dromedarius*. The p4 has a clear lingual wall in the single available specimens of *C. thomasi* and *C. knoblochi*.

Character 12, molarisation of p4: 1) *Megacamelus merriami* (AMNH F23216), not molarized; 2) *Camelus bactrianus* (MNHN.ZM.1971-50), molarized; 3) *Camelus thomasi* (MNHN TER-1685), molarized.

13, 14) in younger species of *Camelus*, the molars are narrower at their base, both relative to the width of P4, and relative to their length, than in early forms.

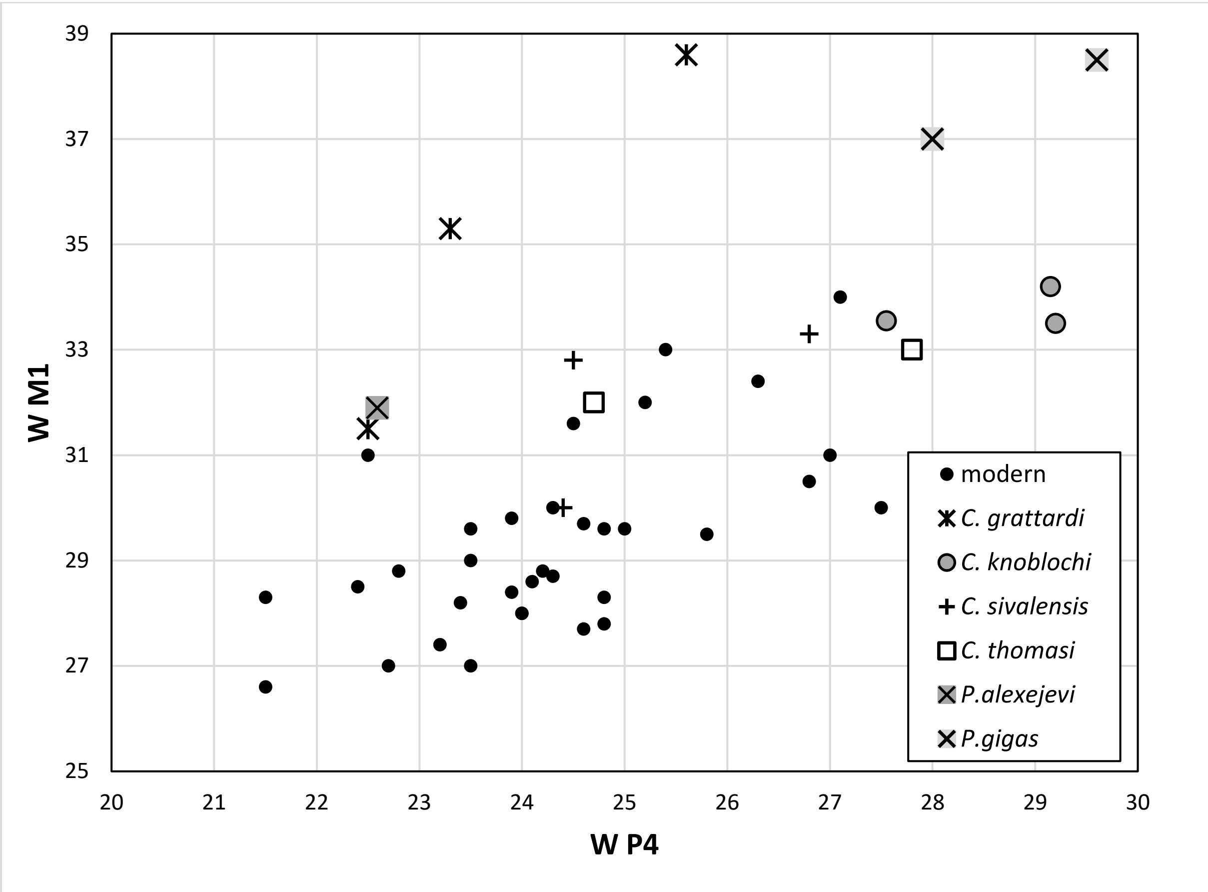

Character 13, relative widths of P4 and M1 (raw data in Supplementary Information 3).

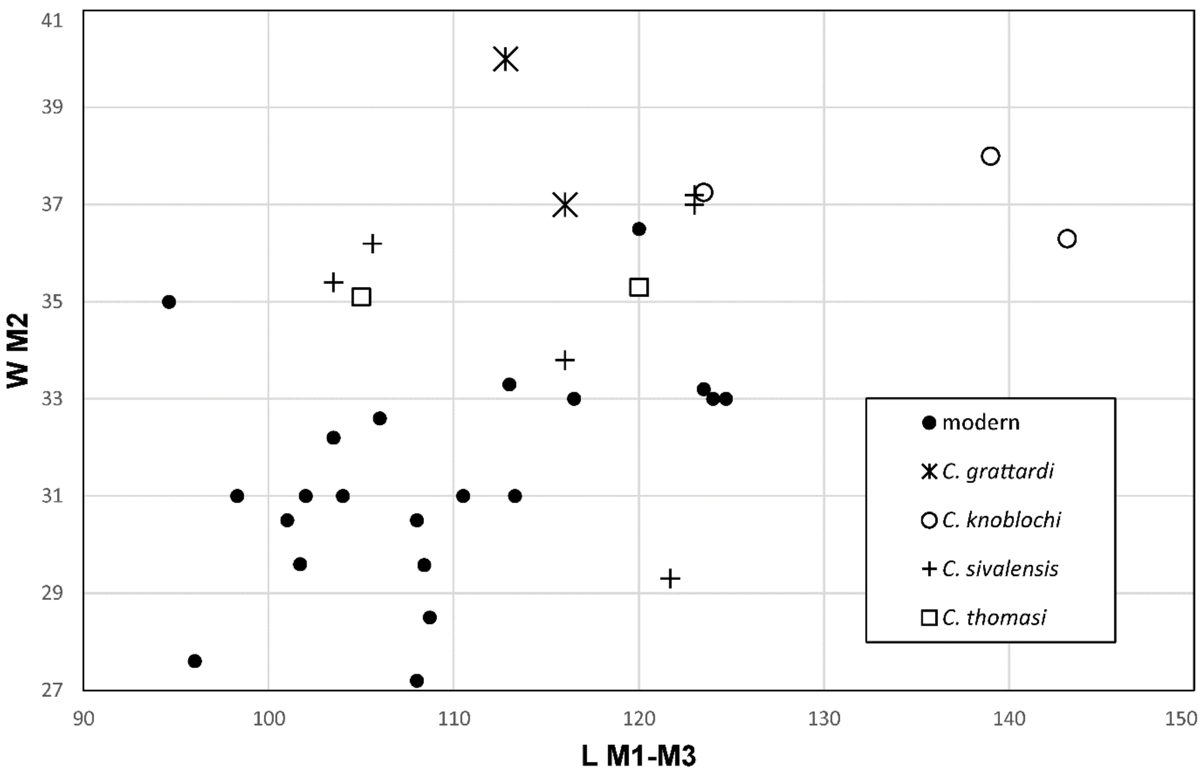

Character 14, width of M2 relative to length of M1–M3 (raw data in Supplementary Information 3).

15) upper molars ribs (labial central pillars on the paracone and metacone) are weak in most *Camelus*, but they are better marked in *C. sivalensis*, in *P. alexejevi*, in a number of isolated finds possibly attributable to *Paracamelus* (Orlov 1929, pl.42, fig.3; van der Made & Morales 1999, fig. 22.1; Rybczynski *et al*. 2013, fig.3c), and in the N. American *M. merriami* and *Aepycamelus major* (but they are distinctly weaker in *Megatylopus*).

16) upper molar styles are usually more reduced in younger species of *Camelus*, although there is significant variation, especially with wear.

Characters 15-16, upper molar ribs and styles. 1) *Megacamelus merriami* (AMNH F23202), strong; 2) *Camelus bactrianus* (MNHN 1970-44), weak; 3) *Camelus sivalensis* (NHMUK PV OR 3664), strong.

17) Geraads (2014) showed that the distal articulation of the humerus of *C. grattardi*, like that of other early forms, is more nearly perpendicular to the long axis of the bone than that of modern ones.

18) the astragalus provides several distinctive criteria, but most of them display high intra-specific variation. The lateral lip of the proximal trochlea extends farther towards the plantar side in the dromedary than in the Bactrian camel, and only *C. thomasi* is similar to the latter.

Character 18, plantar extent of the lateral tibial lip. 1) *Megacamelus merriami* (AMNH FM104232), long; 2) *Camelus dromedarius*, long 3) *Camelus bactrianus*, short; 4) *Camelus thomasi* (MNHN TER-1656), short.

19) in *C. dromedarius*, the cuboid facet is relatively wider than in *C. bactrianus* (Steiger 1990; Martini *et al.* 2017); there is much variation in other taxa, but *P. gigas* (Zdansky 1926, pl. 4, fig. 11) and *P. alexejevi* (Khaveson 1954, pl. 7, fig. 5) are similar to the dromedary.

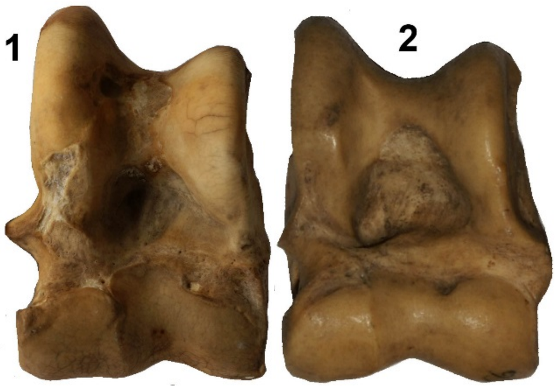

Character 19, width of the cuboid facet 1) *Camelus dromedarius*, broad 2) *Camelus bactrianus*, narrow

20) on the palmar/plantar side of the proximal phalanges, the ligament scars of the proximal end extend farther distally in geologically younger species than in earlier forms, including *P. aguirrei* from Venta del Moro (van der Made & Morales 1999, fig. 22.3), and the Plio-Pleistocene Yukon camel (Rybczynski *et al.* 2013); however, according to Zdansky (1926), *P. gigas* has long scars.

Character 20, length of the ligament scars on the proximal phalanges. 1) *Megacamelus merriami* (AMNH FM104251), short; 2) modern *Camelus*, long; 3) *C. sivalensis* (AMNH FM19832), short; 4) *C. thomasi* (MNHN TER-1674), long.

21) Khaveson (1954) observed that the distal part of the limbs in *P. alexejevi* is relatively longer than in modern forms. *Camelus sivalensis* and *M. merriami* also have long metapodials, while *P. gigas*, instead, is more similar to *C. dromedarius* in this regard, *C. bactrianus* being the most different in its short metapodials.

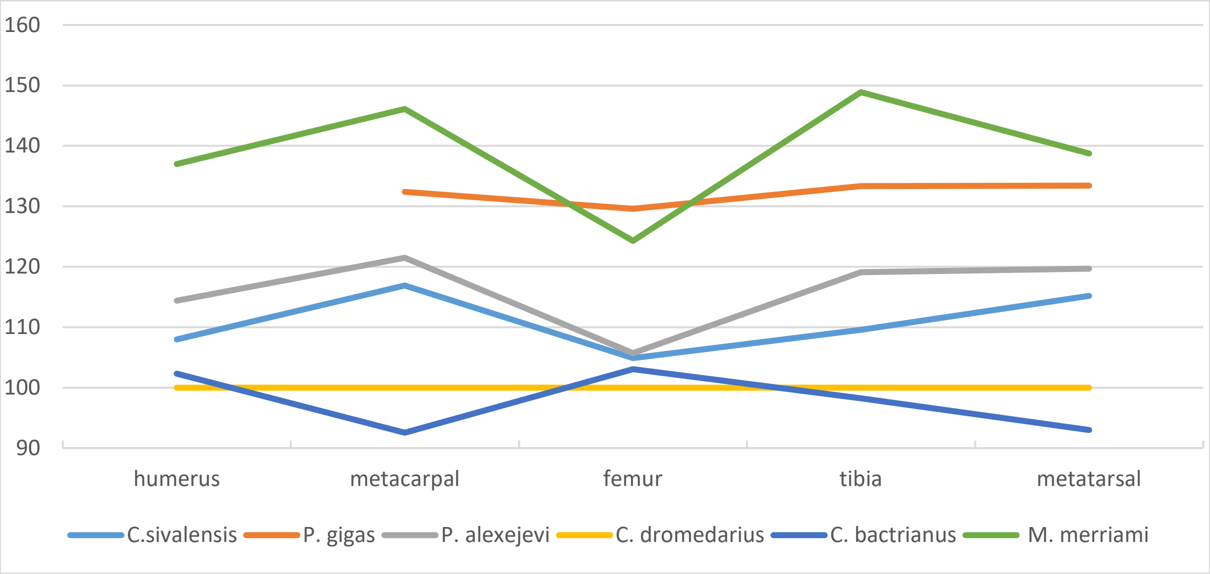

Character 21. Relative length of some long bones (*Camelus dromedarius* = 100). The metatarsal is short relative to the femur in *C. bactrianus*, moderately long in *C. dromedarius* and *P. gigas*, and long in *M. merriami*, *P. alexejevi*, and *C. sivalensis*.

Characters not used:

A) Cranial proportions are hard to evaluate, because most fossil crania are distorted and/or largely reconstructed. *Camelus* crania are clearly broader over the orbits than the well-preserved cranium of *Megatylopus* AMNH-FM14071, but probably not broader than those of the distorted crania of *Megacamelus*.

B) As observed by Zdansky (1926), it is only in *Megatylopus* (AMNH-FM14071) that the lachrymal bone reaches the lachrymal vacuity, which is much larger than in the other taxa.

C) A possible synapomophy of modern *Camelus* is the early fusion of facial sutures; by contrast, they are still clearly visible in adults of *Megacamelus merriami*. However, the condition in many fossil species is too uncertain for a reliable use of this feature.

D) The skull of *Camelus sivalensis* AMNH-FM19832 is unique in having a I3 located far from the canine but the variability of this feature and the condition in most fossil species are unknown.

E) The position of the orbit relative to the tooth-row is very variable in modern forms, and no fossil specimen is outside this variation. Khaveson (1954) stated that it is more posterior in *P. alexejevi*, but this is based upon a largely reconstructed cranium.
F) the proportions of the occiput display much intra-specific variations, but it does look less broad in *C. grattardi* than in other taxa. If so, the condition in this species is autapomorphic.
G) Khaveson largely based his new subgenus *Neoparacamelus*, based upon *P. alutensis*, on the absence on goat folds in lower molars, but this is hard to understand, because a goat fold is clearly present on the m3 of the type specimen (cast in UCBL). The goat fold is frequent in Camelidae but is never strongly expressed.
H) *C. grattardi* is clearly less hypsodont than other *Camelus* (the original material of *C. thomasi* includes an unworn M3, and several specimens of *C. sivalensis* preserve exposed unworn molars), but the degree of hypsodonty is often hard to evaluate with precision, because the base of unworn molars is still embedded in bone. In addition, the slight hypsodonty of the outgroup *M. merriami* is obviously a derived feature, and its use would invert the polarity.
I) In the astragalus, the size of the lateral spine is a good distinguishing feature between living species, but is too variable to be reliably used in fossils.
J) the lateral and plantar calcanear facets are usually contiguous in modern *C. bactrianus* and in *C. thomasi*, but never (5 specimens) in *M. merriami*; they are also separate in NME-MLP-1189, but there is too much intra-specific variation for this character to be used.
K) the proximolateral calcanear facet reaches distally the distolateral facet in *M. merriami*, but not in Old World camels. However the proximolateral facet is short in South-American Camelidae, suggesting that the contact in *M. merriami* is merely an effect of its large size.
L) The unfused part of the metapodials is on the average longer in specimens assigned to *Paracamelus* (*P. gigas*: Zdansky 1926, pl. 2, fig. 10 and pl. 4, fig.15; Teilhard de Chardin & Trassaert 1937, pl. 1, fig. 4; *P. alexejevi*: Baigusheva 1971, pl. 6, fig. 2; Svistun 1971, fig. 1; Titov & Logvynenko, 2006, fig. 5c) than in *Camelus*, but there is much variability in species of both genera (*P. gigas*: Zdansky 1926, pl. 2, fig. 13; *P. alexejevi*: Khaveson 1954, pl. 6; an early Pliocene metatarsal from Chad assigned to *P. gigas* [Likius *et al.* 2003, fig. 3] has a short unfused part).

Matrix and character list, in TNT format:

xread
'Camelidae'
22 10

M_merriami 2 0 2 0 1 0 0 1 0 0 0 0 0 0 0 0 0 0 1 0 0 2
C_grattardi 1 ? 2 0 0 0 0 0 0 1 1 0 ? 0 0 1 0 ? 1 1 0 ?
C_dromedarius 1 1 0 1 1 1 0 1 0 1 1 0 0 2 1 1 1 1 1 2 1 1
C_bactrianus 1 0 1 1 1 1 0 1 1 1 1 0 1 2 1 1 1 1 0 0 1 0
C_sivalensis 1 0 1 ? 0 1 0 0 0 1 1 1 1 1 0 0 0 0 1 0 0 2
C_knoblochi 2 1 2 1 1 1 0 1 1 1 1 0 2 2 1 1 1 1 ? 0 ? ?
C_thomasi 1 0 1 1 1 1 0 0 2 1 1 1 2 1 0 1 0 ? 0 0 1 ?
P_gigas 2 0 1 1 ? 0 1 0 0 0 0 0 0 ? 0 0 0 ? 1 2 1 1
P_alexejevi 1 ? 1 0 ? 0 1 0 0 0 0 ? 0 0 0 0 0 0 ? 2 ? 2
P_alutensis 0 ? ? ? ? ? 1 0 1 0 0 ? 0 ? ? 0 ? 0 ? ? ? ?
;

ccode +[0.21
;
cnames
{ 0 size small medium large ;
{ 1 choanae V-shaped U-shaped ;
{ 2 infra-orbital_shelf narrow moderate broad ;
{ 3 squamosal_reaches_orbital_level yes no ;
{ 4 supra-orbital_foramina wide_apart close ;
{ 5 paraglenoid_tubercle at_most_weak distinct ;
{ 6 length_c-m1/length_m1-m3 short long ;
{ 7 ramus_ascendens oblique vertical ;
{ 8 mandibular_thickening no slight strong ;
{ 9 p3_present absent ;
{ 10 P3_relative_to_P4 large small ;
{ 11 P3_internal_crescent incomplete complete ;
{ 12 p4_molarisation no variable yes ;
{ 13 WP4/WM1 narrow intermediate broad ;
{ 14 molar_breadth/length broad narrow ;
{ 15 upper_molars_ribs moderate weak ;
{ 16 upper_molars_styles strong weak ;
{ 17 distal_humerus transverse oblique ;
{ 18 astragalus_lateral_lip short long ;
{ 19 astragalus_cuboid_facet narrow variable broad ;
{ 20 scars_on_proximal_phalanges short long ;
{ 21 metapodials_relative_to_femur short intermediate long ;

number	**origin**	**taxon**	**W M2**	**L M1-M3**
			modern	modern
1951-102	MNHN	*C. bactrianus*	33,3	101
1896-2017	MNHN	*C. bactrianus*	33	113
no # 2	MNHN	*C. bactrianus*	36,5	124
1974-60	MNHN	*C. bactrianus*	31,9	105
1991-695	MNHN	*C. bactrianus*	33	118,5
1962-183	MNHN	*C. bactrianus*	33,2	116,5
1970-44	MNHN	*C. bactrianus*	31	123,5
1985-243	MNHN	*C. bactrianus*	32,8	110,5
1972-35	MNHN	*C. bactrianus*	31,5	118
1985-1900	MNHN	*C. dromedarius*	30,5	100,5
2007-1438	MNHN	*C. dromedarius*	28	108
1991-302	MNHN	*C. dromedarius*	31	107,4
1931-101	MNHN	*C. dromedarius*	32,6	104
1929-46	MNHN	*C. dromedarius*	28,5	106
1912-442	MNHN	*C. dromedarius*	27,6	108,7
1934-59	MNHN	*C. dromedarius*	31	96
1912-151	MNHN	*C. dromedarius*	31	98,3
2007-1432	MNHN	*C. dromedarius*	31	102
1985-202	MNHN	*C. dromedarius*	33	113,3
1964-213	MNHN	*C. dromedarius*	35	124,7
1865-1	MNHN	*C. dromedarius*	30,8	94,6
1852-564	MNHN	*C. dromedarius*	31	108,7
1897-337	MNHN	*C. dromedarius*	29,6	104
5000-2064	MNHN	*C. dromedarius*	32,2	106,3
5000-2065	MNHN	*C. dromedarius*	29,58	103,5
5000-2068	MNHN	*C. dromedarius*	27,2	111,5
5000-2069	MNHN	*C. dromedarius*	30,5	108
			C. grattardi	*C. grattardi*
Omo75s-70-956	NME	*C. grattardi*	40	112,8
MLP-1346	NME	*C. grattardi*	37	116
			C. thomasi	*C. thomasi*
TER 1816	MNHN	*C. thomasi*	35,1	105
TER 1689	MNHN	*C. thomasi*	35,3	120
			C. knoblochi	*C. knoblochi*
ZIN 8678	Titov, 2008	*C. knoblochi*	38	139
ROMK	Titov, 2008	*C. knoblochi*	37,25	123,5
VSEGEI	Titov, 2008	*C. knoblochi*	36,3	143,15
			C. sivalensis	*C. sivalensis*
36664	NHMUK	*C. sivalensis*	37	123
15347	NHMUK	*C. sivalensis*	35,4	103,5
16405	NHMUK	*C. sivalensis*	33,8	116
PUA Rh 23/83		*C. sivalensis*	29,3	121,7
FM19832	AMNH	*C. sivalensis*	36,2	105,6
FM19785	AMNH	*C. sivalensis*	37,2	123

number	origin	taxon	Height of the medial side
			C. grattardi
MLP-1189	NME	*C. grattardi*	79
			C. sivalensis
NHMUK42564	NHMUK	*C. sivalensis*	75
NHMUK40593	NHMUK	*C. sivalensis*	63
NHMUK40597	NHMUK	*C. sivalensis*	81,7
			C. thomasi
MNHN-TER-1669	MNHN	*C. thomasi*	79
MNHN-TER-1670	MNHN	*C. thomasi*	75
			P. gigas
	Zdansky, 1926	*P. gigas*	88,5
			M. merriami
FM104232	AMNH	*M. merriami*	82,7
FM104231	AMNH	*M. merriami*	89,5
FM104236	AMNH	*M. merriami*	81,8
FM104234	AMNH	*M. merriami*	83
FM104230	AMNH	*M. merriami*	88,5
			C. bactrianus
1851-466	MNHN	*C. bactrianus*	65,7
1898-239	MNHN	*C. bactrianus*	71,5
1926-151	MNHN	*C. bactrianus*	70
1971-50	MNHN	*C. bactrianus*	71,3
1972-35	MNHN	*C. bactrianus*	67,7
MHNG ARCO 826.20-1501.1	Martini et al., 2017	*C. bactrianus*	64,75
NMB 2430	Martini et al., 2017	*C. bactrianus*	68
MHNG MAMO 1168.053	Martini et al., 2017	*C. bactrianus*	71
NMB 10390	Martini et al., 2017	*C. bactrianus*	70,75
NMB 5918	Martini et al., 2017	*C. bactrianus*	66
NMBE 1023261	Martini et al., 2017	*C. bactrianus*	64
ZM 20382	Martini et al., 2017	*C. bactrianus*	69
MSNM Ma 6415	Martini et al., 2017	*C. bactrianus*	67,5
MHNG MAMO 1063.089	Martini et al., 2017	*C. bactrianus*	76,75
MHNG MAMO 810.035	Martini et al., 2017	*C. bactrianus*	72
MHNG ARCO 826.20-1501.2	Martini et al., 2017	*C. bactrianus*	71,5
NBM 10902	Martini et al., 2017	*C. bactrianus*	68
			C. dromedarius
1892-15	MNHN	*C. dromedarius*	76
1876-259	MNHN	*C. dromedarius*	61,8
1884-2210	MNHN	*C. dromedarius*	70
1895-387	MNHN	*C. dromedarius*	63
1899-96	MNHN	*C. dromedarius*	71,2
2007-1435	MNHN	*C. dromedarius*	69,8
1925-205	MNHN	*C. dromedarius*	67
Ek2	Martini et al., 2017	*C. dromedarius*	63,5
Ek3	Martini et al., 2017	*C. dromedarius*	68
MHNG MAMO 78.028	Martini et al., 2017	*C. dromedarius*	62,5
ZM 13130	Martini et al., 2017	*C. dromedarius*	65
Ek5	Martini et al., 2017	*C. dromedarius*	71
MHNG ARCO 826.20-1502.6	Martini et al., 2017	*C. dromedarius*	66,5
MHNG ARCO 826.20-1502.4	Martini et al., 2017	*C. dromedarius*	67,5
NMBE 1023266	Martini et al., 2017	*C. dromedarius*	65,5

Distal breadth
C. grattardi
51,5
C. sivalensis
53,4
46
59,6
C. thomasi
59,5
54,5
P. gigas
62
M. merriami
67
63
63
60
65
C. bactrianus
48,3
50
53,5
48,6
53,7
47
51
50
50,5
47
49
47,5
46,5
57,5
49,5
51
51
C. dromedarius
55
45,5
52,5
47,5
52,5
51
52,5
44
50
45
50
54
48
48
51,5

number	origin	taxon	L M1-M3	W between sup-orb. Foramina
			C. bactrianus	*C. bactrianus*
1951-102	MNHN	*C. bactrianus*	101	50
1896-2017	MNHN	*C. bactrianus*	113	37
no # 2	MNHN	*C. bactrianus*	124	55
1971-50	MNHN	*C. bactrianus*	120	50
1974-60	MNHN	*C. bactrianus*	105	37
1991-695	MNHN	*C. bactrianus*	118,5	56
1962-183	MNHN	*C. bactrianus*	116,5	52,5
1970-44	MNHN	*C. bactrianus*	123,5	60
1985-243	MNHN	*C. bactrianus*	110,5	52
1972-35	MNHN	*C. bactrianus*	118	53
			C. dromedarius	*C. dromedarius*
1985-1900	MNHN	*C. dromedarius*	100,5	26
2007-1437	MNHN	*C. dromedarius*	89	18
1991-302	MNHN	*C. dromedarius*	107,4	48
1912-150	MNHN	*C. dromedarius*	106	12
1929-46	MNHN	*C. dromedarius*	106	21
1912-442	MNHN	*C. dromedarius*	108,7	37
1934-59	MNHN	*C. dromedarius*	96	38
1912-151	MNHN	*C. dromedarius*	98,3	48
2007-1432	MNHN	*C. dromedarius*	102	42
1985-202	MNHN	*C. dromedarius*	113,3	40
1964-213	MNHN	*C. dromedarius*	124,7	48
1865-1	MNHN	*C. dromedarius*	94,6	37
1897-337	MNHN	*C. dromedarius*	104	32
5000-2063	CCEC	*C. dromedarius*	106,5	45
5000-2064	CCEC	*C. dromedarius*	106,3	38,5
5000-2065	CCEC	*C. dromedarius*	103,5	33
5000-2066	CCEC	*C. dromedarius*	108,4	31,5
5000-2067	CCEC	*C. dromedarius*	111,5	27,3
5000-2068	CCEC	*C. dromedarius*	111,5	21,5
5000-2069	CCEC	*C. dromedarius*	108	36,5
1908-101	MNHN	hybrid	120	42
			C. grattardi	*C. grattardi*
MLP-1346	NME	*C. grattardi*	116	66
			C. thomasi	*C. thomasi*
TER 1816	MNHN	*C. thomasi*	105	46
			C. sivalensis	*C. sivalensis*
36664	NHMUK	*C. sivalensis*	123	64
			M. merriami	*M. merriami*
23202	AMNH	*M. merriami*	140	58
23202A	AMNH	*M. merriami*	155	60

number	origin	taxon	L m1-m3	L c-m1	
			C. bactrianus	*C. bactrianus*	
1951-102	MNHN	*C. bactrianus*	111	106	
1896-2017	MNHN	*C. bactrianus*	113	130	
1971-50	MNHN	*C. bactrianus*	130	132,5	
1974-60	MNHN	*C. bactrianus*	116	112	
1991-695	MNHN	*C. bactrianus*	112	137,3	
1962-183	MNHN	*C. bactrianus*	123	132	
1970-44	MNHN	*C. bactrianus*	131	137,5	
1985-243	MNHN	*C. bactrianus*	108	131	
1926-151	MNHN	*C. bactrianus*	130	138	
1972-35	MNHN	*C. bactrianus*	124,6	130	
			C. dromedarius	*C. dromedarius*	
2007-1437	MNHN	*C. dromedarius*	115	118	
1991-302	MNHN	*C. dromedarius*	115	120	
1912-150	MNHN	*C. dromedarius*	115	110	
1929-46	MNHN	*C. dromedarius*	116	115	
1912-442	MNHN	*C. dromedarius*	123	128	
1934-59	MNHN	*C. dromedarius*	101	115	
1912-151	MNHN	*C. dromedarius*	111	112	
2007-1432	MNHN	*C. dromedarius*	110	108	
1985-202	MNHN	*C. dromedarius*	120	125	
1964-213	MNHN	*C. dromedarius*	130	133,5	
1865-1	MNHN	*C. dromedarius*	99	132	
1852-564	MNHN	*C. dromedarius*	114	136,5	
1897-337	MNHN	*C. dromedarius*	111	120	
5000-2063	CCEC	*C. dromedarius*	111	130	
5000-2064	CCEC	*C. dromedarius*	108	130	
5000-2065	CCEC	*C. dromedarius*	106	109	
5000-2066	CCEC	*C. dromedarius*	112,5	128	
5000-2067	CCEC	*C. dromedarius*	115	114	
5000-2068	CCEC	*C. dromedarius*	111,5	122	
5000-2069	CCEC	*C. dromedarius*	113	116	
			P. alutensis	*P. alutensis*	
FSL 17886 (cast of holotype)	Université Claude Bernard, Lyon	*P. alutensis*	96,5	145	
			P. alexejevi	*P. alexejevi*	
OGUM 3267	Khaveson, 1954	*P. alexejevi*	129,5	168	approximate, measured on photograph
OGUM 3271	Khaveson, 1954	*P. alexejevi*	133	180	approximate, measured on photograph
			P. gigas	*P. gigas*	
Loc.11-12987	Teilhard and Trassaert, 1937	*P. gigas*	135	194	approximate, measured on photograph
			C. knoblochi	*C. knoblochi*	
VSEGEI 7/2942		*C. knoblochi*	146	155	approximate, measured on photograph
			C. sivalensis	*C. sivalensis*	
NHMUK 17558	NHMUK	*C. sivalensis*	135	135	
			M. merriami	*M. merriami*	
FM 23216	AMNH	*M. merriami*	151	182	

number	origin	taxon	thickness at m1-m2	H at m1-m2	
			C. bactrianus	*C. bactrianus*	
MNHN-1951-102	MNHN	*C. bactrianus*	34,4	48,2	
MNHN-1896-2017	MNHN	*C. bactrianus*	34,5	40,8	
MNHN-no# 2	MNHN	*C. bactrianus*	35,7	53,1	
MNHN-1971-50	MNHN	*C. bactrianus*	41,4	55	
MNHN-1974-60	MNHN	*C. bactrianus*	34,2	53,3	
MNHN-1898-239	MNHN	*C. bactrianus*	32,7	50,7	
MNHN-1991-695	MNHN	*C. bactrianus*	35	48,3	
MNHN-1962-183	MNHN	*C. bactrianus*	36,3	48,5	
MNHN-1970-44	MNHN	*C. bactrianus*	34,7	57,7	
MNHN-1985-243	MNHN	*C. bactrianus*	35	53,9	
MNHN-1926-151	MNHN	*C. bactrianus*	39	52,7	
MNHN-1972-35	MNHN	*C. bactrianus*	36,7	47	
NMB 5918	Martini et al., 2017	*C. bactrianus*	33,5	54,5	
ZM 20382	Martini et al., 2017	*C. bactrianus*	36,5	55	
NMBE 1023261	Martini et al., 2017	*C. bactrianus*	32,5	41	
NMB 5270	Martini et al., 2017	*C. bactrianus*	33	58,5	
NMB 10390	Martini et al., 2017	*C. bactrianus*	35,5	42,5	
ZM 17970	Martini et al., 2017	*C. bactrianus*	40,5	60	
ZM 17685	Martini et al., 2017	*C. bactrianus*	36,5	59,5	
ZM 17950	Martini et al., 2017	*C. bactrianus*	37	58	
ZM 16783	Martini et al., 2017	*C. bactrianus*	38	54,5	
NMB 2430	Martini et al., 2017	*C. bactrianus*	37	57,5	
ZM 16784	Martini et al., 2017	*C. bactrianus*	37	51	
			C. dromedarius	*C. dromedarius*	
MNHN-1876-259	MNHN	*C. dromedarius*	28	48,1	
MNHN-2007-1437	MNHN	*C. dromedarius*	29	44,9	
MNHN-1991-302	MNHN	*C. dromedarius*	33	49,8	
MNHN-1931-101	MNHN	*C. dromedarius*	34	48,1	
MNHN-1912-150	MNHN	*C. dromedarius*	27,5	49	
MNHN-1929-46	MNHN	*C. dromedarius*	30,5	52,3	
MNHN-1912-442	MNHN	*C. dromedarius*	28,3	50,5	
MNHN-1934-59	MNHN	*C. dromedarius*	28	52,9	
MNHN-1912-151	MNHN	*C. dromedarius*	29,5	51,2	
MNHN-2007-1432	MNHN	*C. dromedarius*	33	47,9	
MNHN-1985-202	MNHN	*C. dromedarius*	40	50,2	
MNHN-1964-213	MNHN	*C. dromedarius*	36	49,4	
MNHN-1865-1	MNHN	*C. dromedarius*	32	55,4	
MNHN-1925-205	MNHN	*C. dromedarius*	33	54,6	
MNHN-1852-564	MNHN	*C. dromedarius*	30	50,8	
MNHN-1897-337	MNHN	*C. dromedarius*	30,4	48,4	
5000-2063	CCEC, Lyon	*C. dromedarius*	28	52	
5000-2064	CCEC, Lyon	*C. dromedarius*	36	55,5	
5000-2065	CCEC, Lyon	*C. dromedarius*	35	47,3	
5000-2067	CCEC, Lyon	*C. dromedarius*	33,5	49,3	
5000-2069	CCEC, Lyon	*C. dromedarius*	26,8	49	
Ek1	Martini et al., 2017	*C. dromedarius*	30,5	53	
NMB 1022	Martini et al., 2017	*C. dromedarius*	31	54	
ZM 13130	Martini et al., 2017	*C. dromedarius*	30	56	
Ek3	Martini et al., 2017	*C. dromedarius*	29	56,7	
NMB 1583	Martini et al., 2017	*C. dromedarius*	27	56,5	
ZM 13620	Martini et al., 2017	*C. dromedarius*	34	59,5	
ZM 14499	Martini et al., 2017	*C. dromedarius*	31	58,5	
ZM 10811	Martini et al., 2017	*C. dromedarius*	28	55,5	
NMB 2128	Martini et al., 2017	*C. dromedarius*	30,5	52,5	
ZM 10812	Martini et al., 2017	*C. dromedarius*	35	47,5	
Ek5	Martini et al., 2017	*C. dromedarius*	29	58,5	
			C. thomasi	*C. thomasi*	
TER 1683	MNHN	*C. thomasi*	39	37	
TER 1684	MNHN	*C. thomasi*	38	36	
TER 1685	MNHN	*C. thomasi*	41,5	39,5	
TER 1687	MNHN	*C. thomasi*	43,5	39	
TER 1688	MNHN	*C. thomasi*	35,8	43	
TER 1900-27	MNHN	*C. thomasi*	45	43	
			M. merriami	*M. merriami*	
FM 23216	AMNH	*M. merriami*	43	81	
			C. grattardi	*C. grattardi*	
Omo L4807	NME	*C. grattardi*	30	45	approximate measurements
			C. sivalensis	*C. sivalensis*	
AMNH19832	AMNH	*C. sivalensis*	29,5	74	
NHMUK 100163 (4	NHMUK	*C. sivalensis*	30	50	
NHMUK 17558	NHMUK	*C. sivalensis*	42,5	56	
NHMUK 39599	NHMUK	*C. sivalensis*	35	61	
NHMUK16165	NHMUK	*C. sivalensis*	32	69	
			P. alutensis	*P. alutensis*	
FSL 17886 (cast of holotype)	Université Claude Bernard, Lyon	*P. alutensis*	27,2	35,7	
			P. gigas	*P. gigas*	
18911	Teilhard and Trassaert, 1937	*P. gigas*	35	57	approximate, measured on photograph
	Zdansky, 1926	*P. gigas*	41	89	approximate, measured on photograph
KB3.97.316, Chad	CAR, N'Djamena	*P. gigas*	33	58	approximate measurements

number	origin	taxon	W P4	W M1
			modern	modern
1896-2017	MNHN	*C. bactrianus*	26,8	30,5
no # 2	MNHN	*C. bactrianus*	27,1	34
1971-50	MNHN	*C. bactrianus*	25,4	33
1974-60	MNHN	*C. bactrianus*	24,3	30
1991-695	MNHN	*C. bactrianus*	24,8	28,3
1962-183	MNHN	*C. bactrianus*	24,6	29,7
1970-44	MNHN	*C. bactrianus*	27	31
1985-243	MNHN	*C. bactrianus*	24,8	29,6
1972-35	MNHN	*C. bactrianus*	25,2	32
1876-259	MNHN	*C. dromedarius*	22,4	28,5
1985-1900	MNHN	*C. dromedarius*	24,6	27,7
2007-1438	MNHN	*C. dromedarius*	23,5	27
1991-302	MNHN	*C. dromedarius*	25	29,6
1931-101	MNHN	*C. dromedarius*	22,8	28,8
1912-150	MNHN	*C. dromedarius*	21,5	26,6
1929-46	MNHN	*C. dromedarius*	23,5	29
1912-442	MNHN	*C. dromedarius*	22,7	27
1934-59	MNHN	*C. dromedarius*	23,2	27,4
1912-151	MNHN	*C. dromedarius*	24,1	28,6
2007-1432	MNHN	*C. dromedarius*	24,3	28,7
1985-202	MNHN	*C. dromedarius*	27,5	30
1964-213	MNHN	*C. dromedarius*	26,3	32,4
1865-1	MNHN	*C. dromedarius*	24,2	28,8
1852-564	MNHN	*C. dromedarius*	21,5	28,3
1897-337	MNHN	*C. dromedarius*	24,8	27,8
2007-1435	MNHN	*C. dromedarius*	23,9	28,4
5000-2064	CCEC	*C. dromedarius*	24,5	31,6
5000-2065	CCEC	*C. dromedarius*	23,5	29,6
5000-2066	CCEC	*C. dromedarius*	23,4	28,2
5000-2067	CCEC	*C. dromedarius*	25,8	29,5
5000-2068	CCEC	*C. dromedarius*	23,9	29,8
5000-2069	CCEC	*C. dromedarius*	24	28
5000-2070	CCEC	*C. dromedarius*	22,5	31
1908-101	MNHN	*C. dromedarius*	24	28
			C. grattardi	*C. grattardi*
Omo75s-70-956	NME	*C. grattardi*	25,6	38,6
MLP-1346	NME	*C. grattardi*	23,3	35,3
			C. thomasi	*C. thomasi*
TER 1816	MNHN	*C. thomasi*	24,7	32
TER 1689	MNHN	*C. thomasi*	27,8	33
			P. alexejevi	*P. alexejevi*
mean	Logvynenko, 2000	*P. alexejevi*	22,59	31,9
			P. gigas	*P. gigas*
22192	Teilhard and Trassaert, 1937	*P. gigas*	28	37
	Zdansky, 1926	*P. gigas*	29,6	38,5
			C. knoblochi	*C. knoblochi*
ZIN 8678	Titov, 2008	*C. knoblochi*	29,2	33,5
ROMK	Titov, 2008	*C. knoblochi*	27,55	33,55
VSEGEI	Titov, 2008	*C. knoblochi*	29,15	34,2
			C. sivalensis	*C. sivalensis*
36664	NHMUK	*C. sivalensis*	26,8	33,3
15347	NHMUK	*C. sivalensis*	24,5	32,8
16405	NHMUK	*C. sivalensis*	24,4	30
PUA Rh 23/83	Gaur et al., 1984	*C. sivalensis*	19,6	28
FM19832	AMNH	*C. sivalensis*	21,3	34,2

	length of long bones				
	C. sivalensis	*P. gigas*	*P. alexejevi*	*C. dromedarius*	*C. bactrianus*
reference	AMNH FM 19832	Zdansky, 1926	Logvynenko, 2000; mean	Martini et al., 2017; mean	Martini et al., 2017; mean
humerus	420		426	389	398
metacarpal	408	462	425	349	323
femur	514	635	518	490	505
tibia	493	600	518	450	442
metatarsal	410	475	429	356	331

P. merriami
Harrison, 1985
533
510
609
670
494

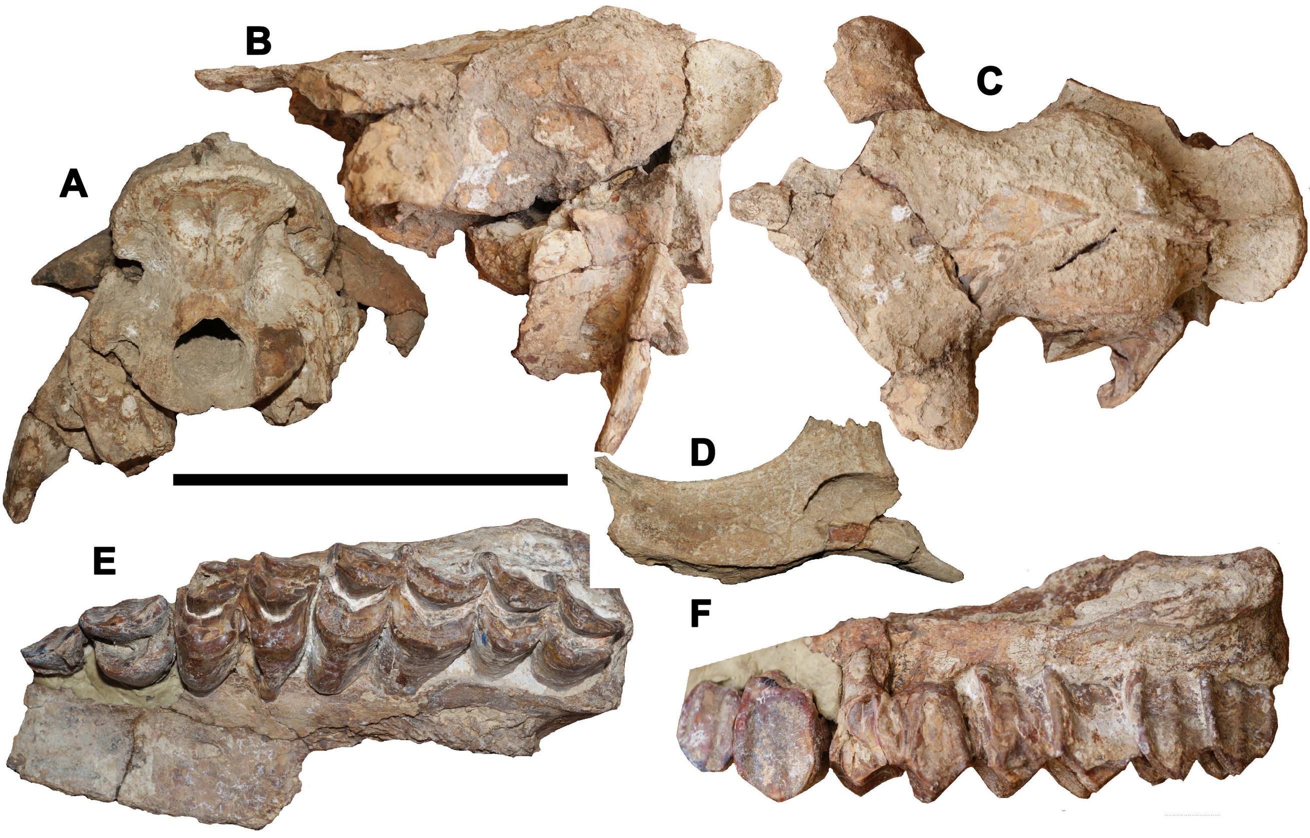

A
B
C
D
E
F

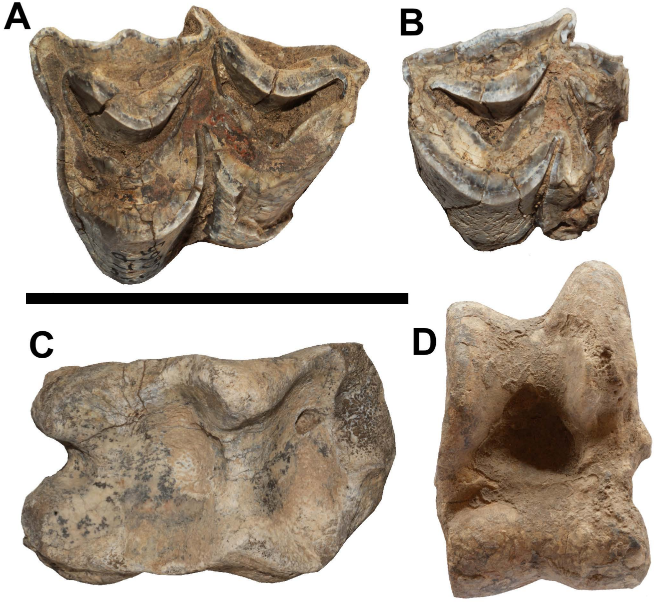
A
B
C
D

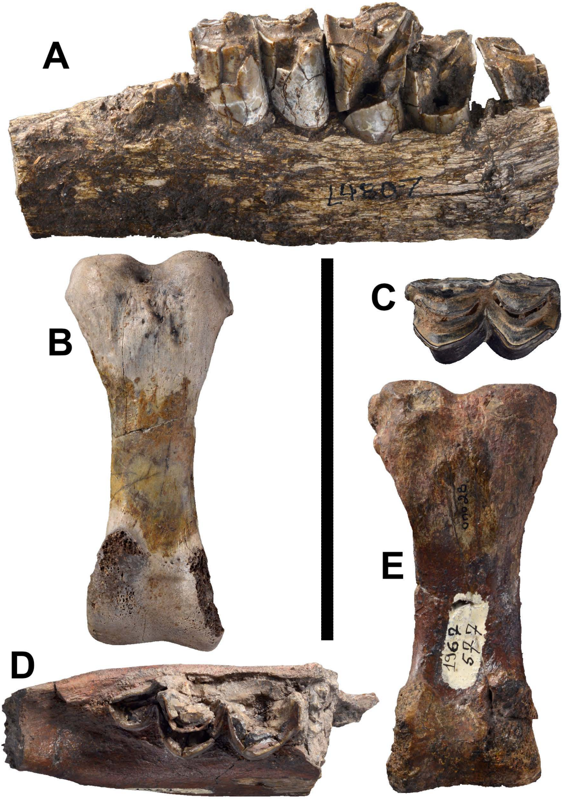
A
L4807
B
C
D
E

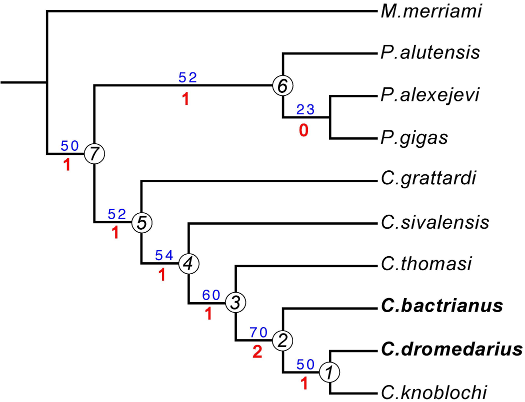

M.merriami
P.alutensis
P.alexejevi
P.gigas
C.grattardi
C.sivalensis
C.thomasi
C.bactrianus
C.dromedarius
C.knoblochi
52
1
6
23
0
50
1
7
52
1
5
54
1
4
60
1
3
70
2
2
50
1
1

Table 1. Dental measurements of NME-MLP-1346 (L = length; W = width).

LP3	WP3	LP4	WP4	LM1	WM1	LM2	WM2	LM3	WM3	M1−M3
21	15	24	23	37	35	44	37	43.2	30+	116

Table 2. Tooth height in some *Camelus*; height of unworn molars cannot be measured in most specimens, because their base is concealed in bone. Height of unworn teeth is underlined.

	C. grattardi		*C. dromedarius*	*C. sivalensis*			*C. thomasi*
	NME-MLP-1346		extant	NHMUK			type
			N=3	40570	40561	15357	
Tooth	P3	P4	P3	P3	M1	M2	M3
Length	21	24	mean 17.4	19.8	50.3	54.4	39
Height	24.2	33	26–30	28++	58	62	50+